# Article

# Complexin Maintains Vesicles in the Primed State in *C. elegans*

Robert J. Hobson,[1,2] Qiang Liu,[1,2] Shigeki Watanabe,[1] and Erik M. Jorgensen[1,*]
[1]Howard Hughes Medical Institute and Department of Biology, University of Utah, Salt Lake City, UT 84112, USA

## Summary

**Background:** Complexin binds the SNARE complex at synapses and regulates exocytosis, but genetic studies indicate contradictory roles: in flies it predominantly inhibits synaptic vesicle fusion, whereas in mice it promotes evoked responses.
**Results:** Here we characterize the complexin mutant in the nematode *Caenorhabditis elegans* and reveal bipolar functions in neurotransmission: complexin inhibits spontaneous fusion of synaptic vesicles but is also essential for evoked responses. Complexin mutants exhibit a doubling of vesicle fusion in the absence of extracellular calcium. Even more profoundly, mutants exhibit an almost complete loss of evoked responses, and current amplitudes are reduced by 94%. One possible interpretation is that complexin is required for the stabilization of docked vesicles and that, in its absence, vesicles may fuse or undock from the plasma membrane. Consistent with this hypothesis, docked synaptic vesicles are reduced by 70% in *complexin-1* mutants.
**Conclusion:** These data suggest that the main function of complexin is to maintain the docked state both by inhibiting fusion and by promoting priming.

## Introduction

During constitutive secretion, vesicles fuse to the cell membrane and release their cargo. Membrane fusion is mediated by the intertwining of SNARE proteins anchored in the plasma and vesicle membranes [1]. The SNARE complex also mediates exocytosis of synaptic vesicles, with SNARE protein interactions forming the primed state. However, the fusion process is interrupted, and primed vesicles are held in a ready state until there is a stimulus. When the neuron is depolarized, calcium flows in through voltage-gated ion channels and relieves the block. Thus, regulated secretion requires a brake to block fusion and a calcium sensor to relieve the block. Synaptotagmin contains C2 domains capable of binding calcium and phospholipids, and it is widely accepted that synaptotagmin acts as the calcium sensor in synaptic vesicle fusion [2, 3]. What protein interrupts fusion and holds vesicles in the docked state? Although synaptotagmin could also play an inhibitory role in fusion, recent studies suggest that another SNARE-interacting protein, complexin, may be responsible for blocking constitutive exocytosis [4–7]. Complexin forms an α helix that binds in the groove between syntaxin and synaptobrevin across the middle two-thirds of the SNARE complex and stabilizes the complex [8]. However,

both biochemical and genetic experiments designed to test complexin function are contradictory, and the role of complexin in calcium-driven fusion remains controversial.

In liposome and whole-cell fusion assays, complexin blocks fusion [9, 10]. Complexin appears to block fusion by interfering with SNARE zippering [11, 12]. The block is relieved by the addition of synaptotagmin and calcium [9, 10, 13, 14]. A couple of biochemical assays suggest that complexin might facilitate fusion [15, 16]. In these assays, complexin was capable of increasing the rate of SNARE-mediated liposome fusion, possibly by stabilizing the SNARE complex [8]. Despite these studies, the predominant activity observed for complexin in biochemical studies is to inhibit exocytosis.

By contrast, analysis of mutants indicates that the predominant activity of complexin is to promote exocytosis. In autaptic synapses from mutant mice lacking *complexin-1* and *complexin-2*, evoked release was reduced by 66% [17] and miniature postsynaptic currents were reduced by 30% [18]. Similarly, loss of complexin in *Drosophila* results in an approximately 40% reduction in evoked release [19, 20].

Paradoxically, genetic studies in *Drosophila* also suggest that complexin blocks exocytosis. In these mutants, synaptic vesicles fuse to the plasma membrane constitutively. This increase in rate is due in part to a role in development: fly mutants exhibit a doubling of the number of active zones. However, the increase in the rate of spontaneous vesicle fusion is much larger, nearly 20-fold [19, 20]. Knockdown of *complexin-1* and *complexin-2* by RNA interference (RNAi) in mouse cortical neurons caused a 4-fold increase in spontaneous release [12], but the increase in spontaneous release is not observed in the mouse complexin knockouts [18]. It is not clear why the knockdown and knockout experiments in mice exhibit opposite effects on spontaneous vesicle fusion, but these results underscore the contradictory nature of complexin in synaptic vesicle fusion.

Here we characterize complexin knockouts in the nematode *Caenorhabditis elegans*. We demonstrate that *complexin-1* plays both facilitatory and inhibitory roles in synaptic vesicle exocytosis at the neuromuscular junction. Evoked release is largely absent in *cpx-1* mutants, whereas tonic fusions are increased. These defects are accompanied by a severe decrease of docked vesicles at the synapse.

## Results

### The *cpx-1* Isoform Functions at the Nematode Neuromuscular Junction

Two complexin genes, *cpx-1* and *cpx-2*, are predicted in the *C. elegans* genome (Figure 1A; see also Figures S1 and S2 available online). Worm *cpx-1* exhibits greater identity to the fly and mouse complexins than *cpx-2* (39% identity between CPX-1 and mouse complexin-1 versus 32% identity between CPX-2 and mouse complexin-1 (Figure 1; Figure S2). For CPX-1, highest conservation is observed in the central helical domain (75%), which binds the SNARE complex, whereas the N-terminal facilatory domain, the accessory domain, and the C-terminal domains each exhibit about 30% identity. The domains of complexin are defined based on

*Correspondence: jorgensen@biology.utah.edu
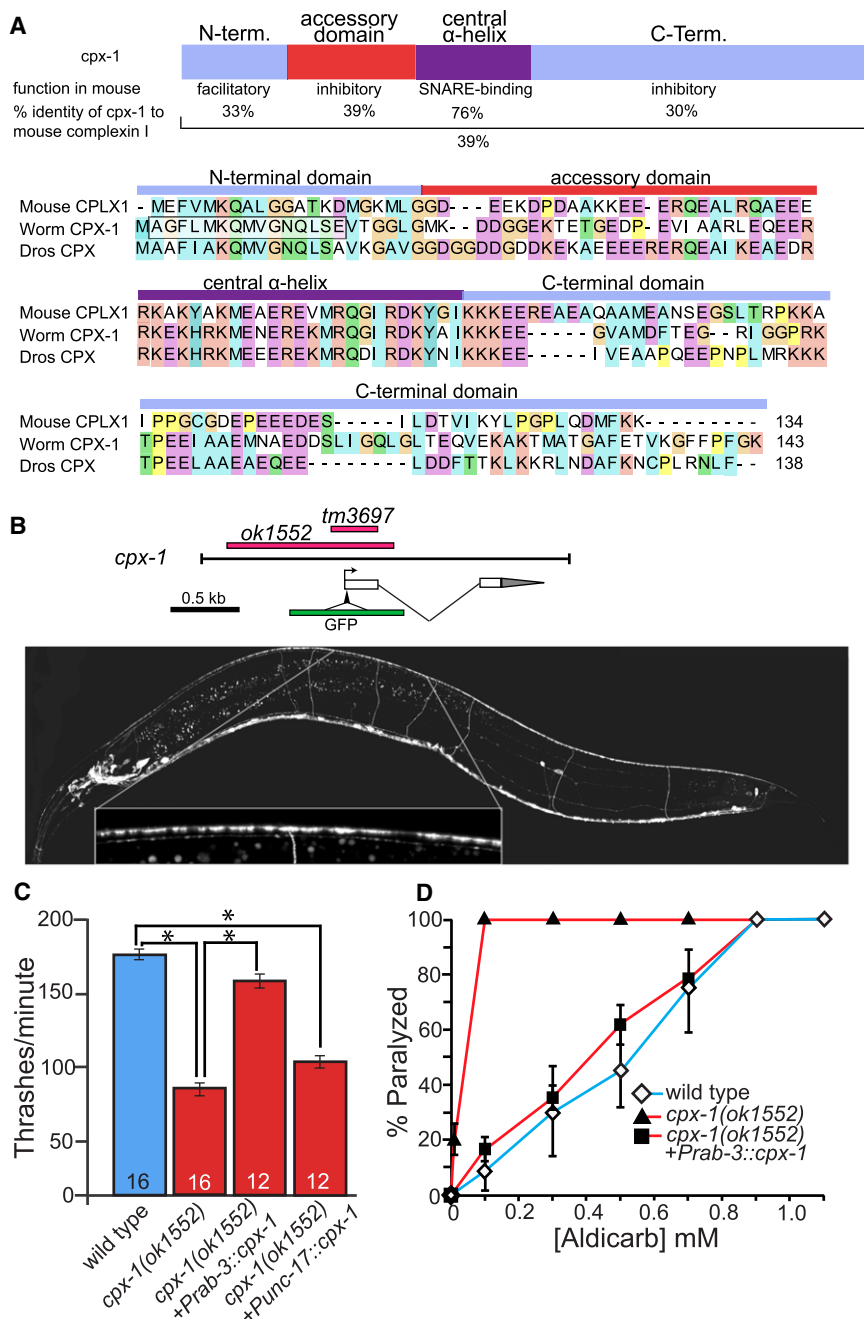[2]These authors contributed equally to this work

Figure 1. *cpx-1* Encodes the Worm Homolog of Complexin and Regulates Locomotion and Neurotransmitter Release

(A) *cpx-1* is the complexin gene with the highest identity to mouse and fly complexins. *C. elegans* CPX-1 was aligned with mouse CplxI (AAH14803) and fly complexin (AAF69518) using ClustalW2. Percent identities were calculated using Jalview [33].

(B) *cpx-1* is expressed in the nervous system. Top: gene model and regions deleted in *C. elegans* complexin mutant alleles (red bars). The black line represents the region of the genome used to create the rescuing GFP construct. Gray triangle on transcript represents the 3′UTR. GFP was inserted after the first three codons. Bottom: a reporter construct consisting of the *cpx-1* gene with GFP inserted at the N terminus of complexin is expressed in many neurons in the head and body of the animal. Neurons expressing *cpx-1* include the motor neurons of the ventral nerve cord, neurons in the head ganglia, and also neurons of the pharyngeal nervous system, including the MC and M4 motorneurons. The inset shows the punctate localization of GFP::CPX-1 along the dorsal nerve cord. Confocal images were taken of young adult hermaphrodites oriented dorsal up and anterior to the left. Images are a stitch of multiple confocal Z projections along the length of the animal.

(C) *cpx-1* mutants are defective for thrashing in liquid. *cpx-1* thrashing behavior can be rescued by expressing *cpx-1* under a panneuronal promoter (P*rab-3::cpx-1* EG4633), but not by expressing it specifically in the acetylcholine neurons (P*unc-17::cpx-1* EG4713). Graph shows means and standard error of the mean (SEM) of the thrashing behavior. Tukey-Kramer multiple comparisons test: *p < 0.001. The n values for each strain are listed at the bottom of each bar.

(D) *cpx-1* mutants are hypersensitive to the acetylcholinesterase inhibitor aldicarb, indicating that excessive acetylcholine is released at neuromuscular junctions. This sensitivity can be rescued by expressing *cpx-1* in all neurons using the *rab-3* promoter. Graph shows means and SEM.

(tm1871) mutants are viable and grow to adulthood; similarly, *cpx-1(ok1552) cpx-2(tm1871)* double mutants develop into fertile adults.

Nevertheless, *cpx-1(ok1552)* mutants are uncoordinated. To quantify body movement, we performed thrashing assays. Animals placed in a drop of water will swim by rapid reciprocal contractions of the body; locomotory activity can be quantified by counting flexures. Wild-type animals are capable of maintaining high rates of thrashing, whereas *cpx-1(ok1552)* worms exhibit reduced thrashing in liquid (Figure 1C). *cpx-2(tm1871)* mutants exhibit no swimming defect, suggesting that *cpx-1*, but not *cpx-2*, is important for the regulation of locomotion (Figure S2). To test whether loss of complexin results in defective neurotransmission, we tested the sensitivity of the complexin mutants to the acetylcholinesterase inhibitor aldicarb. Loss of *cpx-1*, but not *cpx-2*, resulted in hypersensitivity to aldicarb, suggesting that there is excessive neurotransmitter release at the neuromuscular junction

sequence conservation across multiple animal phyla (see Figure S1 legend for full description of how the domains were defined). To assay for complexin function at neuromuscular junctions, we analyzed mutations in *cpx-1* and *cpx-2*. *cpx-1(ok1552)* deletes the first of two exons of the gene, which includes the N terminus, the accessory domain, the central helix, and part of the C-terminal domain. *cpx-2(tm1871)* deletes part of the accessory domain, the central helix, and part of the C-terminal domain of *cpx-2* (Figure 1B; Figure S2). Complexins in mice and *Drosophila* are required for viability; *complexin-1 complexin-2* double knockout mice die a few hours after birth, and complexin null flies die before adult eclosion [17, 19]. By contrast, *C. elegans cpx-1(ok1552)* and *cpx-2*
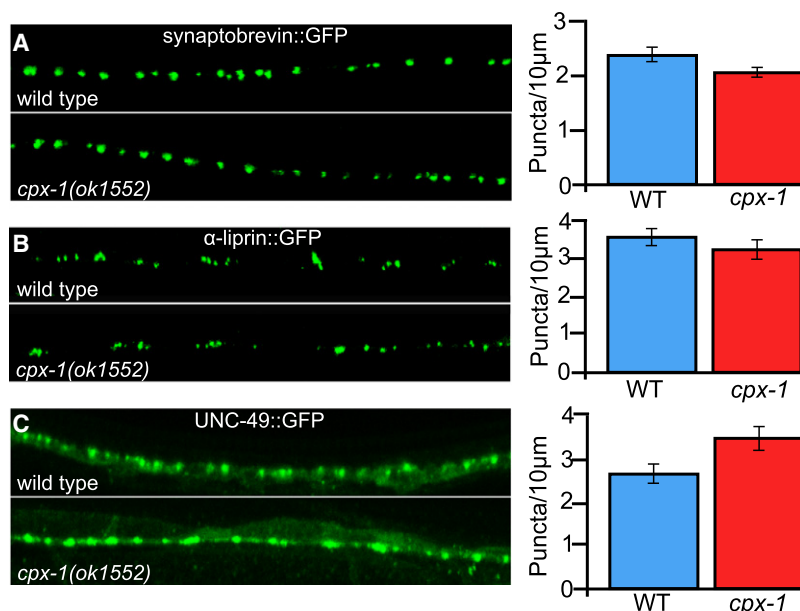
**Figure 2. cpx-1 Mutants Exhibit Normal Presynaptic and Postsynaptic Morphology**

Left: sample image of each synaptic reporter. Images for all strains were taken of the dorsal nerve cord near the posterior gonad reflex. Right: quantification of the number of GFP-positive puncta per 10 μm. Ten images were analyzed for each strain.

(A) cpx-1 mutation does not affect the number of synaptic vesicle clusters visualized by synaptobrevin::GFP (nIs52).

(B) Normal numbers of synapses are observed in cpx-1 mutants, as visualized by the dense projection marker α-liprin::GFP (hpIs3).

(C) GFP-tagged GABA receptors (oxIs22) are clustered normally at postsynaptic sites. Images are confocal Z stacks of a 70 μm section of the dorsal nerve cord. n = 10 sections of dorsal nerve cord for each strain. All graphs show means and SEM for the number of punctae per 10 μm.

(Figure 1D; Figure S2). The thrashing and aldicarb hypersensitivity phenotypes of cpx-1 mutants can be fully rescued by expressing the cpx-1 gene under its own promoter or under a panneuronal promoter, demonstrating that complexin is functioning in the nervous system (Figure 1D; Figure S3). The aldicarb hypersensitivity defect can also be rescued by expressing cpx-1 in just the acetylcholine neurons, demonstrating that excess neurotransmitter release arises from a cell-autonomous defect in the motor neurons (Figure S3A). However, thrashing was not rescued by expressing cpx-1 specifically in the acetylcholine motor neurons, suggesting that cpx-1 is required more broadly in the nervous system for normal locomotion (Figure 1C). cpx-1 cpx-2 double mutants are not more severe than the cpx-1 single mutant for the thrashing or aldicarb assays, demonstrating that cpx-1 plays the dominant role for the locomotory phenotypes (Figure S2). Together, these data suggest that cpx-1 functions in the motor neurons to prevent excess neurotransmitter release.

Complexins in other species are expressed mostly in neuronal tissue [4–6, 19]. To determine the expression pattern of the C. elegans complexin genes, we tagged the N termini of CPX-1 and CPX-2 with GFP. Each fusion construct includes the promoter, all introns, and the native 3′ untranslated region (UTR) (Figure 1B; Figure S2). The cpx-1 transgenic reporter is widely expressed in the nervous system, including all the ventral cord motor neurons (Figure 1B). The CPX-1 protein is clustered into puncta along the dorsal and ventral nerve cords, suggesting that the protein is likely localized to synapses (Figure 1B, inset). Because the transgene rescues the cpx-1 aldicarb hypersensitivity phenotype, the tagged protein is functional (Figure S3). Because no obvious phenotype was detected for cpx-2, it was not possible to assay rescue. However the expression pattern suggests that cpx-2 is more narrowly expressed, including in a few neurons in the head and tail ganglia and in the coelomocyte scavenger cells, but not in the motor neurons of the ventral nerve cord (Figure S2). The expression patterns and behavioral phenotypes suggest that cpx-1 is the primary complexin functioning at neuromuscular junctions.

### Loss of cpx-1 Has Contradictory Effects on Synaptic Transmission

Loss of complexin results in a developmental defect in Drosophila neurons: the numbers of synaptic varicosities and active zones are nearly doubled [19]. It is has been suggested that the increase in tonic release leads to synaptic hypertrophy in Drosophila. To determine whether there is a developmental defect at C. elegans synapses, we examined synaptic markers in cpx-1(ok1552) mutants. Normal numbers of neuromuscular junctions were observed in cpx-1 mutants, as assayed by counting synaptic vesicle clusters (synaptobrevin-GFP) or dense projections (α-liprin/SYD-2::GFP) along the ventral nerve cord (Figures 2A and 2B). Normal postsynaptic receptor fields were observed in cpx-1 mutants by labeling the muscle GABA receptor (UNC-49::GFP; Figure 2C). Finally, axon outgrowth appeared to be normal in cpx-1 (ok1552) mutants, as determined by labeling the GABA motor neurons (Figure S3). It is possible that the synaptic phenotypes of cpx-1 mutants arose from long-term compensatory changes that occurred during development. To examine a developmental role for cpx-1, we expressed cpx-1(+) under the control of two different heat-shock promoters in cpx-1(ok1552) mutant animals (Figure S3). In the absence of heat shock, the transgenes failed to rescue the aldicarb hypersensitivity of cpx-1 (ok1552); after heat shock, in adult animals, normal aldicarb sensitivity was restored. Taken together, these results suggest that the development of the nervous system in a cpx-1 mutant is grossly normal and that the uncoordinated phenotype and hypersensitivity to aldicarb are due to defects in synaptic function rather than an increase in synaptic number.

Hypersensitivity to aldicarb suggests excessive neurotransmitter release at the neuromuscular junction. Three mechanisms of neurotransmitter release could be responsible for the increase: evoked, tonic, or spontaneous release. Evoked release is generated by an action potential or a depolarizing stimulus from an electrode. The transient depolarization causes an influx of calcium at the synapse and stimulates the fusion of vesicles in the readily releasable pool. The coherent release of neurotransmitter produces a large postsynaptic current. Tonic release occurs even in the absence of a stimulus. If the membrane potential of the neuron at rest is sufficiently depolarized, a low level of calcium influx leads to sporadic vesicle fusion and miniature postsynaptic
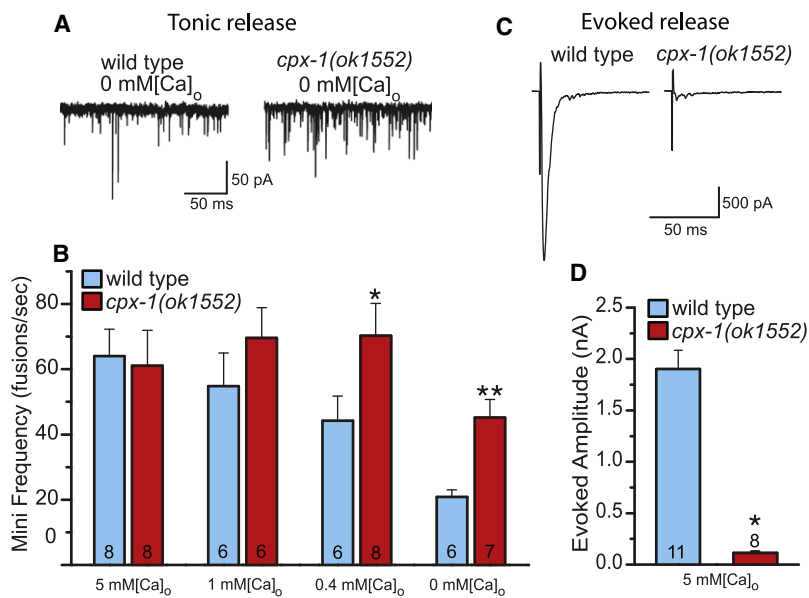
Figure 3. *cpx-1* Mutants Exhibit Elevated Spontaneous Fusion and Reduced Evoked Responses

(A) Representative traces of wild-type and *cpx-1(ok1552)* miniature postsynaptic currents (minis) from unstimulated motor neurons at 0 mM calcium.

(B) Tonic neurotransmitter release at varying calcium concentrations. Each miniature current represents the fusion of a single synaptic vesicle. The increased frequency of miniature currents in *cpx-1* mutants at 0 mM extracellular calcium suggests that these vesicles may be fusing spontaneously in calcium-independent fusion. Mini frequencies in 5 mM calcium: wild-type 64 ± 8 minis/s, *cpx-1(ok1552)* 61 ± 11 minis/s; in 1 mM calcium: wild-type 55 ± 10 minis/s, *cpx-1(ok1552)* 69 ± 9 minis/s; in 0.4 mM calcium: wild-type 44 ± 7 minis/s, *cpx-1(ok1552)* 70 ± 10 minis/s (*p < 0.05 versus wild-type); in 0 mM calcium: wild-type 21 ± 2 minis/s, *cpx-1(ok1552)* 45 ± 6 minis/s (**p < 0.005 versus wild-type). Probabilities calculated using an unpaired independent t test.

(C) Representative traces of electrically evoked responses at 5 mM calcium of wild-type, *cpx-1(ok1552)*.

(D) Summary of evoked responses from the wild-type (1903 ± 182 nA) and *cpx-1(ok1552)* (113 ± 13 nA). Wild-type versus *cpx-1(ok1552)* p < 0.00001 using an unpaired independent t test. All graphs show means and SEM.

currents. Note that tonic release still requires calcium. In the absence of extracellular calcium, vesicle fusion is very rare and is called spontaneous fusion.

We measured these three types of neurotransmitter release using voltage-clamp recordings from neuromuscular junctions in *cpx-1(ok1552)* mutants [21]. At 5 mM calcium, tonic release in *cpx-1* mutants was the same as in the wild-type (Figures 3A and 3B). Tonic release is sensitive to extracellular calcium, so mini frequencies were measured over a range of calcium concentrations (Figure 3B). To measure spontaneous release, we recorded minis in the absence of extracellular calcium. Note that, even in the absence of extracellular calcium, some minis are observed in *C. elegans*; these residual minis, however, are dependent on calcium from internal stores [22]. Interestingly, the *cpx-1(ok1552)* mutants still exhibited a >40% increase in mini frequency compared to the wild-type at 0 mM calcium. These results suggest that CPX-1 is required to block spontaneous calcium-independent fusion of synaptic vesicles.

To evaluate evoked release, we stimulated the ventral nerve cord with an electrode. Evoked release was reduced by 94% in *cpx-1(ok1552)* animals, demonstrating that the readily releasable pool was almost completely absent (Figures 3C and 3D). Once again, the defect in evoked release could be rescued by expressing *cpx-1(+)* in the nervous system of the mutant strain (Figure 5). These data suggest that in addition to an inhibitory role, complexin is playing a positive role in fusion.

**Complexin Plays Dual Roles in Exocytosis**

One possible interpretation of these data is that complexin plays one role at the synapse: it blocks spontaneous fusion of synaptic vesicles. In this model, the absence of the evoked release is caused by a depletion of primed vesicles by spontaneous fusion. To assay for a depletion of docked vesicles, we examined the number and distribution of synaptic vesicles using electron microscopy. At a gross level, the synapses seem normal in *cpx-1* mutants: the morphology is normal (Figure 4A), synaptic vesicles have a normal diameter (Figure S4C), and vesicles are clustered around the dense projection (Figure S4A). However, the total number of synaptic vesicles is reduced to

about 50% in *cpx-1(ok1552)* mutants compared to the wild-type (Figure 4B). Moreover, the number of docked vesicles is severely reduced: there is a 70% reduction of docked vesicles at acetylcholine synapses and a 75% reduction of docked vesicles at GABA synapses (Figure 4C). Docking at the plasma membrane is reduced along the entire active zone (Figure S4B).

The ultrastructural data are superficially consistent with complexin having a single function: it blocks spontaneous fusion. If this model were true, then one would expect that weak mutations would lead to an increase in spontaneous fusion and a concomitant decrease in evoked release; that is, the phenotypes should always be reciprocal. The first 15 amino acids of murine complexin are required for stimulating neurotransmission [12, 23, 24]. Specifically, the methionine and lysine residues at positions 5 and 6 in mouse complexin are believed to mediate the stimulatory effect [23], and these residues are conserved between mice and worms (Figure 1A). We deleted sequence coding for the 15 amino acids at the N terminus of the complexin gene (ΔN-*cpx-1*; Figure 5A). To ensure that constructs were stable and not overexpressed, we inserted the transgenes as single copies into the *cpx-1 (ok1552)* genome using Mos-mediated single copy insertion [25]. A *cpx-1(+)* gene expressed in neurons rescues the locomotory phenotypes and evoked responses and also inhibits the spontaneous fusion of vesicles (Figures 1C and 1D; Figure 5). The N-terminal deletion construct partially rescues the locomotory phenotype (Figure S5). Electrophysiological recordings demonstrate that spontaneous fusion is increased in the N-terminal deletion allele compared to the wild-type (Figures 5B and 5C), suggesting that the N terminus is required to inhibit spontaneous fusion. Surprisingly, the N-terminal deletion causes an increase rather than a decrease in evoked release (Figures 5D and 5E). These data tell us two important facts about complexin: (1) unlike in the mouse, the N-terminal domain in the worm inhibits fusion, both evoked and spontaneous, and (2) the negative and positive roles of complexin are separable. The N-terminal domain is required to inhibit fusion; the stimulatory functions must reside elsewhere. We conclude that complexin plays dual roles during vesicle fusion.
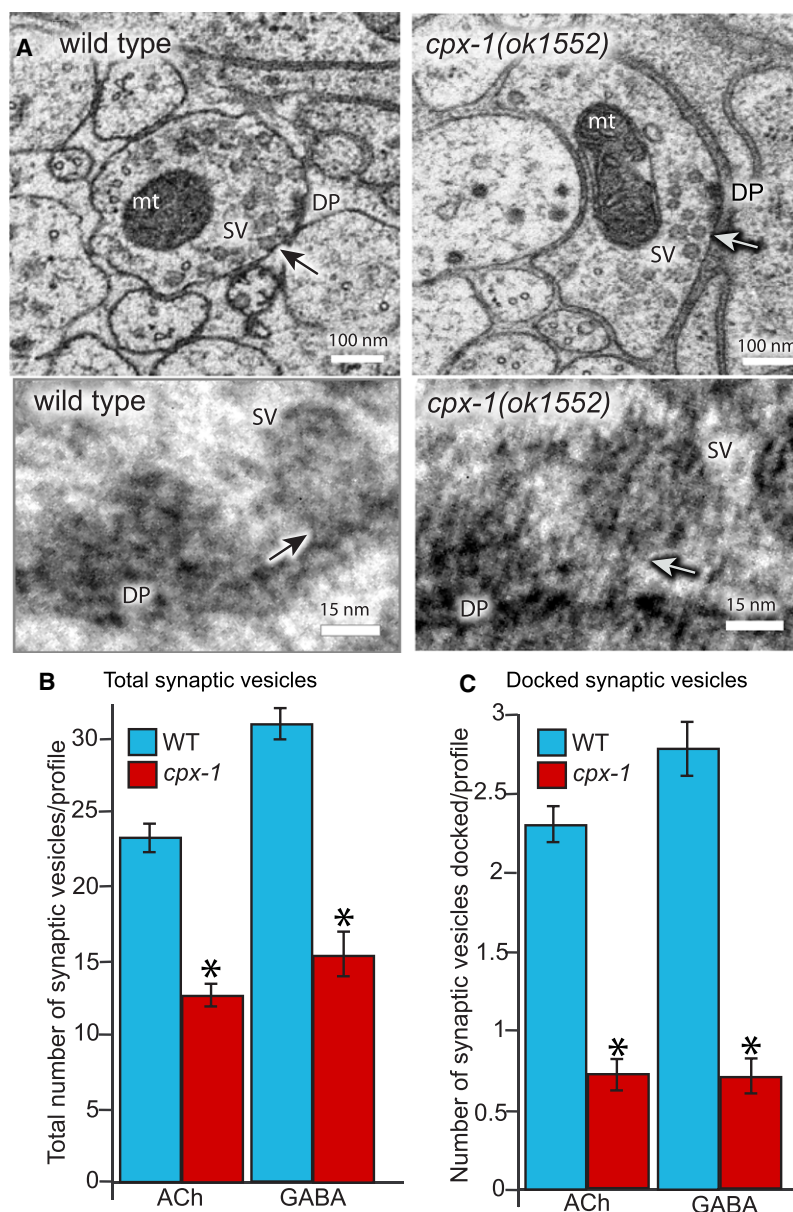
Figure 4. *cpx-1* Mutants Have Reduced Numbers of Synaptic Vesicles at the Synapse

(A) Top: representative electron micrographs of a wild-type and a *cpx-1* neuromuscular junction. The following abbreviations are used: mt, mitochondria; DP, dense projection; SV, synaptic vesicles. Bottom: high-magnification images of a synapse from wild-type (left) and *cpx-1(ok1552)* (right) animals. Left: a vesicle docked to the plasma membrane adjacent to a dense projection at a wild-type neuromuscular junction. The arrow indicates the contact between the vesicle and plasma membrane. Right: a vesicle tethered to the plasma membrane next to the dense projection in a *cpx-1(ok1552)* animal. The arrow indicates the tether connecting the plasma membrane to the vesicle.

(B) Summary of the total number of synaptic vesicles per profile containing a dense projection. Wild-type acetylcholine neurons: 23.3 ± 0.8 vesicles; *cpx-1(ok1552)* acetylcholine neurons: 12.5 ± 0.8 vesicles (p < 0.0001, unpaired t test). Wild-type GABA neurons: 30.9 ± 1.0 vesicles; *cpx-1(ok1552)* GABA neurons: 15.3 ± 1.5 vesicles (p < 0.0001, unpaired t test).

(C) Total number of docked synaptic vesicles per profile containing a dense projection. Docked vesicles: wild-type acetylcholine neurons: 2.3 ± 0.1 vesicles; *cpx-1 (ok1552)* acetylcholine neurons: 0.7 ± 0.1 vesicles (p < 0.0001 unpaired t test). Docked vesicles: wild-type GABA neurons: 2.8 ± 0.2 vesicles; *cpx-1(ok1552)* GABA neurons: 0.7 ± 0.1 vesicles (p < 0.0001 unpaired t test). A vesicle is considered docked if it is contacting the plasma membrane [32]. All graphs show means and SEM.

independent of extracellular calcium. Thus, complexin may inhibit the spontaneous fusion of vesicles from both the evoked and tonic pools. An inhibitory role for complexin in tonic fusion is consistent with observations in both flies and mice. Complexin mutants in *Drosophila* exhibit elevated rates of spontaneous fusion, as measured by field potentials at the neuromuscular junction of third instar larvae [19]. Similarly, knockdown of complexin in mouse cortical neurons by RNA interference led to a 4-fold increase in the rate of spontaneous fusion [12].

An increased consumption of synaptic vesicles should lead to a depletion of vesicles at mutant synapses. In *C. elegans*, spontaneous fusion occurs at high enough levels to deplete both docked and cytoplasmic pools of vesicles, as observed by electron microscopy. There is a 70% decrease in the number of vesicles docked at active zones in *cpx-1* mutants, presumably because vesicles spontaneously fuse after the priming of the SNARE complex. The loss of complexin from the *C. elegans* neuromuscular junction even depletes the reserve pool of vesicles by 50%, indicating that the high rates of fusion are outpacing the ability of the cell to replenish vesicles at the synapse. Although an increase in spontaneous fusion is not observed in mouse knockouts, there is a reduction in the readily releasable pool, i.e., docked and primed vesicles, as measured by applying moderately hyperosmotic media [23].

The inhibitory role of complexin in synaptic vesicle fusion is borne out by biochemical studies of membrane fusion. Complexin can inhibit SNARE-mediated fusion of whole cells [10] and also block SNARE-mediated fusion of liposomes [9]. The block of SNARE-mediated fusion appears to involve the

## Discussion

Contradictory interpretations have been put forward for the role of complexin in synaptic vesicle fusion: some data suggest that complexin blocks spontaneous fusion of synaptic vesicles, and other data suggest that complexin stimulates exocytosis. We find evidence for both of these roles in the nematode *C. elegans*.

### Blocking Fusion

Our data demonstrate that the complexin protein arrests SNARE-mediated fusion. First, in dissected preparations, spontaneous vesicle fusion is increased at *cpx-1* neuromuscular junctions. Second, increased exocytosis occurs in undissected animals as well: complexin mutant animals exhibit an increased sensitivity to aldicarb, a drug that blocks the degradation of acetylcholine. The increased rate of release is not simply an increase in tonic release. Tonic release depends on extracellular calcium, whereas spontaneous release is
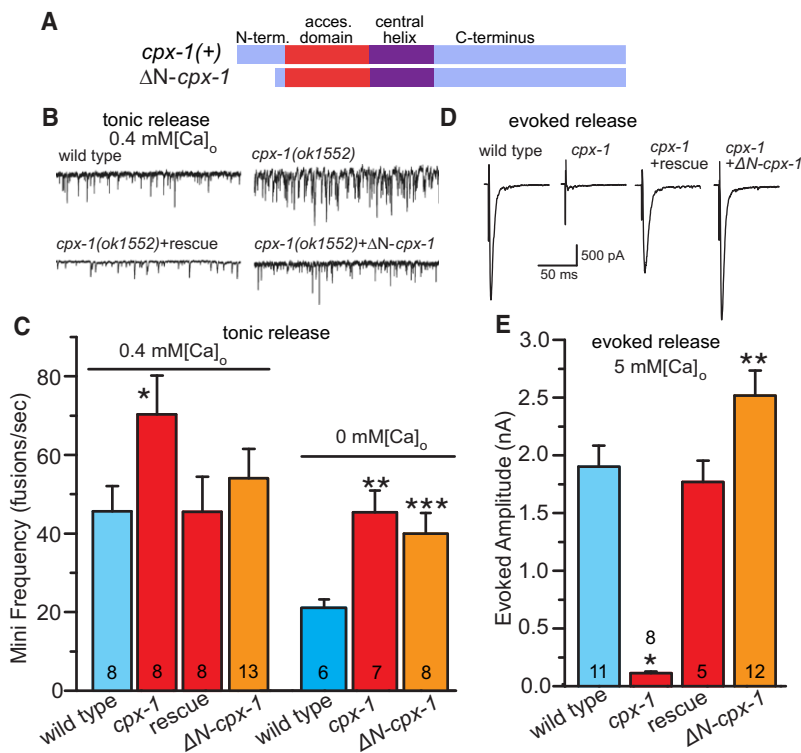
**Figure 5. The N Terminus of cpx-1 Is Not Required for Evoked Release at the C. elegans Neuromuscular Junction**

(A) Models of the wild-type and the N-terminal truncation mutant. The ΔN-cpx-1 mutant truncates the 15 amino acids immediately following the start codon (see box in Figure 1A).

(B) Sample traces of tonic release in 0.4 mM extracellular calcium.

(C) The ΔN-cpx-1 does not rescue the spontaneous release phenotype of cpx-1(ok1552) mutants at 0 mM extracellular calcium. At 0.4 mM calcium, wild-type 46 ± 6 minis/s, cpx-1(ok1552) 70 ± 10 minis/s (*p < 0.05 versus wild-type), cpx-1(ok1552) + rescue (EG4633) 46 ± 9 minis/s, ΔN-cpx-1 (EG6182) 54 ± 7 minis/s. At 0 mM extracellular calcium, wild-type 21 ± 2 minis/s, cpx-1(ok1552) 45 ± 6 minis/s (**p < 0.005 versus wild-type), ΔN-cpx-1 (EG6182) 40 ± 5 minis/s (***p < 0.02 versus wild-type). Wild-type complexin is capable of fully rescuing the null mini frequency.

(D) Sample traces of evoked release from the wild-type, cpx-1(ok1552), cpx-1(ok1552) + rescue (EG4633), cpx-1(ok1552) + ΔN-cpx-1.

(E) Evoked release is rescued in cpx-1(ok1552) mutants by expressing either wild-type complexin or the N-terminal truncation mutant ΔN-cpx-1 in neurons. Wild-type 1903 ± 182 nA, cpx-1(ok1552) 113 ± 13 nA (*p < 0.001), cpx-1(ok1552) + rescue (EG4633) 1768 ± 186 nA, ΔN-cpx-1 (EG6182) 2518 ± 215 nA (**p < 0.05) at 5 mM extracellular calcium. The wild-type and null mutant in (C) and (E) are recapitulated from Figure 3. n values are indicated in the bars. All graphs show means and SEM.

accessory domain of complexin, which may prevent synaptobrevin from fully zippering the SNARE complex [9–11].

## Stimulating Exocytosis

Complexin is also required for calcium-stimulated exocytosis in C. elegans: evoked currents are reduced by 94% in the complexin mutant. These data are also consistent with data from flies and mice. In Drosophila, complexin mutants exhibit an approximately 30%–40% decrease in evoked potential [19]. In mouse cultured neurons, disruption of complexin by mutation or RNAi knockdown causes an approximately 70% decrease in evoked responses compared to the wild-type [12, 17, 18]. Thus, loss of evoked synaptic vesicle exocytosis is a common feature of complexin mutants in all organisms studied.

How can complexin facilitate evoked release when it clearly inhibits spontaneous fusion of synaptic vesicles? There are two possible models for the role of complexin in evoked release. In the first model, complexin has only one function: to inhibit spontaneous vesicle fusion; the defect in evoked release is an indirect effect of depletion of the vesicle pool through spontaneous fusion. In the second model, complexin also has a domain that facilitates evoked release. In short, in this second model, complexin has dual functions: to inhibit spontaneous release of the tonic pool and to facilitate fusion from the evoked pool.

## Stimulating by Inhibiting

In the inhibitory model, rapid consumption of vesicles via spontaneous fusion depletes vesicles from the evoked pool (Figure 6, middle). Thus, a role for complexin in stimulating exocytosis is an illusion of an empty readily releasable pool. An attractive aspect of this model is its simplicity: complexin would have a single, uncomplicated function in synaptic vesicle exocytosis. If this were true, mutations that partially disrupt the inhibitory function should also disrupt stimulatory functions—the phenotypes should always be linked—and increase in spontaneous fusion should result in a proportional reduction in the number of vesicles in the readily releasable pool. By contrast, mutations in the N-terminal domain increase spontaneous release but do not reduce evoked release (Figure 5). In fact, evoked release is even higher than in the wild-type. Similarly, removal of the prenylation motif from Drosophila complexin, deletion of the C-terminal domain, or disruption of the central helix of C. elegans CPX-1 exhibits normal evoked release but increases spontaneous release (Martin et al. [26], this issue of Current Biology) [27]. Together, these data suggest that the synapses in worms and flies can maintain high rates of tonic release without depleting the evoked vesicle pool.

## A Stimulatory Domain

In the dual function model, complexin inhibits spontaneous release from the tonic pool but facilitates evoked release. We found in C. elegans that complexin is essential for evoked release, potentially supporting a dual role for complexin. In the mouse, the N terminus of complexin is required for evoked responses possibly to promote a late step in the fusion process [12, 20, 23]. Surprisingly, when we deleted these residues in C. elegans complexin, evoked release was not disrupted. These data suggest that residues involved in promoting fusion are located in a different region of the molecule than the N terminus in C. elegans.

## Stimulating by Docking

How, then, might complexin facilitate evoked release at a molecular level? An alternative model is that complexin facilitates evoked release via the central helix (Figure 6). The binding of the central helix domain of complexin to the partially zippered
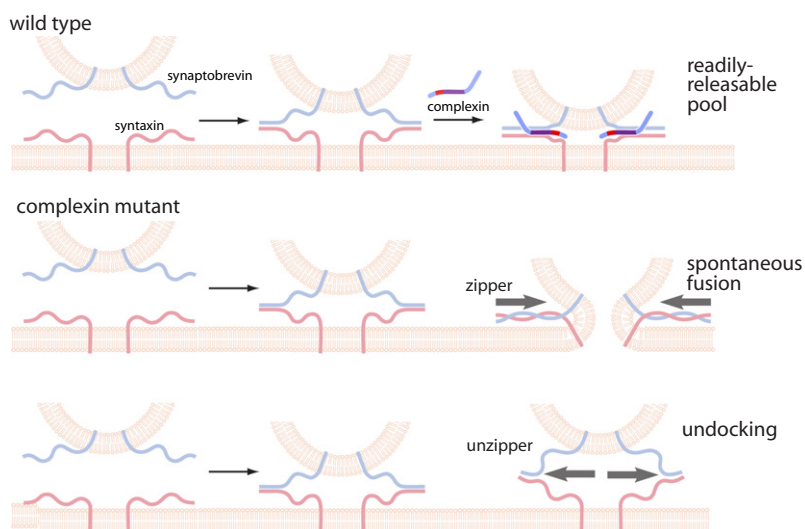
Figure 6. Model for Dual Functions of Complexin

Top: complexin functions to maintain primed vesicles in the readily releasable pool by stabilizing the SNARE complex in a partially zippered state. Middle: in the absence of complexin, the SNAREs can fully zipper and drive membrane fusion, thereby allowing spontaneous fusion. Bottom: in the absence of complexin, the SNAREs might unzipper and reverse the docking of vesicles, thereby depleting evoked responses. Complexin might provide this stabilizing effect on its own or in conjunction with other synaptic proteins. The SNARE protein SNAP-25 is not shown for simplicity.

SNARE complex could prevent unzippering and the reversal of the primed state [7, 8]. In an in vitro vesicle docking assay, binding by complexin stabilizes the *trans* configuration [15]. In the absence of complexin, *trans*-SNARE complexes are reversible, and primed vesicles would become unprimed (Figure 6, bottom). Such reversal of priming would contribute to the reduction of docked vesicles observed at the *C. elegans* neuromuscular junction and account for the unusually severe defect in evoked release. In this model, complexin stabilizes the SNARE complex and hence increases the number of primed vesicles. Again, the elegance of this model is its simplicity: complexin stabilizes the docked state. However, we cannot exclude the possibility that complexin plays a more direct role in evoked release, for example via regulatory interactions with synaptotagmin.

## Species Diversity

How can we reconcile contradictory data for complexin mutants in different experimental systems? In the mouse, complexin primarily stimulates evoked release, whereas in flies it primarily blocks spontaneous release. In the worm, complexin plays a prominent role in both functions: complexin is essential for evoked release, and it blocks spontaneous fusion. However, these differences among species are ones of degree: inhibitory and stimulatory functions for complexin are found in each organism. Given the strong sequence conservation, it is likely that complexin is playing similar roles at all synapses, its character shaped by the other players at the synapse. It seems that complexin encompasses schizophrenic roles in exocytosis: it both blocks and stimulates fusion.

## Experimental Procedures

### Constructs and Strains

All constructs were made using standard molecular biology techniques and Gateway technology (Invitrogen). For a full description of how all constructs were made, see the Supplemental Experimental Procedures. Either rescuing or reporter constructs were microinjected into the worm gonads to produce progeny carrying extrachromosomal arrays or single copy insertions of rescuing or mutant complexins were produced using MosSCI, as previously described [25]. For a full description of the methodologies used to create transgenic *C. elegans*, see the Supplemental Experimental Procedures.

### Behavioral Assays

Thrashing assays were performed as previously described [28] and are fully described in the Supplemental Experimental Procedures. For the aldicarb assays, 20–25 worms were added to the center of room-temperature aldicarb plates and scored for paralysis after 4 hr. The assays are fully described in the Supplemental Experimental Procedures. For heat-shock experiments, strains were heat shocked for 1 hr at 34°C and then allowed to recover at room temperature for 6 hr prior to assay. For heat-shock aldicarb assays, 20–25 worms were added to a plate containing 1 mM aldicarb and scored for paralysis every 15 min.

### Confocal Microscopy

Worms were immobilized in 2% phenoxypropanol in M9 solution on freshly made 2% agarose pads. Images were acquired on a Pascal LSM5 confocal microscope (Zeiss) with a 63× 1.4NA oil objective. For imaging of the dorsal nerve cord, worms were imaged with the dorsal surface facing toward the objective. For each of the synaptic markers, a Z stack was taken of a 70 μm section of nerve cord, and the total number of GFP-positive puncta was counted.

### Electrophysiology

Young adult hermaphrodite animals were used for electrophysiological analysis. Miniature and evoked postsynaptic currents (mPSCs and ePSCs) at the neuromuscular junction were recorded as previously described [21, 29]. For a full description of electrophysiological methods and analysis, see the Supplemental Experimental Procedures. Data were imported into Origin, version 7.5 (OriginLab) for graphing and statistical analysis. Unpaired t test was used for statistical comparisons. $p < 0.05$ is considered statistically significant.

### Electron Microscopy

N2 and *cpx-1(ok1552)* worms were fixed in parallel for electron microscopy using high-pressure freezing followed by substitution of solvent-based fixatives, as previously described [30–32]. For a full description of the electron microscopy methods, see the Supplemental Experimental Procedures.

All morphometry was conducted blind to genotype and included a matched wild-type worm that was fixed in parallel. The number of synaptic vesicles (~30 nm in diameter) in each synaptic profile was counted, and their distances from the dense projection and plasma membrane were measured. Docked vesicles were defined as touching the plasma membrane. Analysis included the acetylcholine neurons VA and VB and the GABA neuron VD.

### Reagents

All chemicals were purchased from Sigma-Aldrich and all molecular reagents from Invitrogen and New England Biolabs, unless otherwise stated. Worm strains not generated in the lab were ordered from the Caenorhabditis Genetics Center (http://www.cbs.umn.edu/CGC/).

### Supplemental Information

Supplemental Information includes five figures, Supplemental Experimental Procedures, and one table and can be found with this article online at doi:10.1016/j.cub.2010.12.015.

**References**

1. Jahn, R., and Scheller, R.H. (2006). SNAREs—engines for membrane fusion. Nat. Rev. Mol. Cell Biol. *7*, 631–643.

2. Geppert, M., Goda, Y., Hammer, R.E., Li, C., Rosahl, T.W., Stevens, C.F., and Südhof, T.C. (1994). Synaptotagmin I: A major Ca2+ sensor for transmitter release at a central synapse. Cell *79*, 717–727.

3. Fernández-Chacón, R., Königstorfer, A., Gerber, S.H., García, J., Matos, M.F., Stevens, C.F., Brose, N., Rizo, J., Rosenmund, C., and Südhof, T.C. (2001). Synaptotagmin I functions as a calcium regulator of release probability. Nature *410*, 41–49.

4. Takahashi, S., Yamamoto, H., Matsuda, Z., Ogawa, M., Yagyu, K., Taniguchi, T., Miyata, T., Kaba, H., Higuchi, T., Okutani, F., et al. (1995). Identification of two highly homologous presynaptic proteins distinctly localized at the dendritic and somatic synapses. FEBS Lett. *368*, 455–460.

5. Ishizuka, T., Saisu, H., Odani, S., and Abe, T. (1995). Synaphin: A protein associated with the docking/fusion complex in presynaptic terminals. Biochem. Biophys. Res. Commun. *213*, 1107–1114.

6. McMahon, H.T., Missler, M., Li, C., and Südhof, T.C. (1995). Complexins: Cytosolic proteins that regulate SNAP receptor function. Cell *83*, 111–119.

7. Pabst, S., Margittai, M., Vainius, D., Langen, R., Jahn, R., and Fasshauer, D. (2002). Rapid and selective binding to the synaptic SNARE complex suggests a modulatory role of complexins in neuroexocytosis. J. Biol. Chem. *277*, 7838–7848.

8. Chen, X., Tomchick, D.R., Kovrigin, E., Araç, D., Machius, M., Südhof, T.C., and Rizo, J. (2002). Three-dimensional structure of the complexin/SNARE complex. Neuron *33*, 397–409.

9. Schaub, J.R., Lu, X., Doneske, B., Shin, Y.K., and McNew, J.A. (2006). Hemifusion arrest by complexin is relieved by Ca2+-synaptotagmin I. Nat. Struct. Mol. Biol. *13*, 748–750.

10. Giraudo, C.G., Eng, W.S., Melia, T.J., and Rothman, J.E. (2006). A clamping mechanism involved in SNARE-dependent exocytosis. Science *313*, 676–680.

11. Giraudo, C.G., Garcia-Diaz, A., Eng, W.S., Chen, Y., Hendrickson, W.A., Melia, T.J., and Rothman, J.E. (2009). Alternative zippering as an on-off switch for SNARE-mediated fusion. Science *323*, 512–516.

12. Maximov, A., Tang, J., Yang, X., Pang, Z.P., and Südhof, T.C. (2009). Complexin controls the force transfer from SNARE complexes to membranes in fusion. Science *323*, 516–521.

13. Tang, J., Maximov, A., Shin, O.H., Dai, H., Rizo, J., and Südhof, T.C. (2006). A complexin/synaptotagmin 1 switch controls fast synaptic vesicle exocytosis. Cell *126*, 1175–1187.

14. Chicka, M.C., and Chapman, E.R. (2009). Concurrent binding of complexin and synaptotagmin to liposome-embedded SNARE complexes. Biochemistry *48*, 657–659.

15. Yoon, T.Y., Lu, X., Diao, J., Lee, S.M., Ha, T., and Shin, Y.K. (2008). Complexin and Ca2+ stimulate SNARE-mediated membrane fusion. Nat. Struct. Mol. Biol. *15*, 707–713.

16. Malsam, J., Seiler, F., Schollmeier, Y., Rusu, P., Krause, J.M., and Söllner, T.H. (2009). The carboxy-terminal domain of complexin I stimulates liposome fusion. Proc. Natl. Acad. Sci. USA *106*, 2001–2006.

17. Reim, K., Mansour, M., Varoqueaux, F., McMahon, H.T., Südhof, T.C., Brose, N., and Rosenmund, C. (2001). Complexins regulate a late step in Ca2+-dependent neurotransmitter release. Cell *104*, 71–81.

18. Xue, M., Stradomska, A., Chen, H., Brose, N., Zhang, W., Rosenmund, C., and Reim, K. (2008). Complexins facilitate neurotransmitter release at excitatory and inhibitory synapses in mammalian central nervous system. Proc. Natl. Acad. Sci. USA *105*, 7875–7880.

19. Huntwork, S., and Littleton, J.T. (2007). A complexin fusion clamp regulates spontaneous neurotransmitter release and synaptic growth. Nat. Neurosci. *10*, 1235–1237.

20. Xue, M., Lin, Y.Q., Pan, H., Reim, K., Deng, H., Bellen, H.J., and Rosenmund, C. (2009). Tilting the balance between facilitatory and inhibitory functions of mammalian and *Drosophila* complexins orchestrates synaptic vesicle exocytosis. Neuron *64*, 367–380.

21. Richmond, J.E., and Jorgensen, E.M. (1999). One GABA and two acetylcholine receptors function at the *C. elegans* neuromuscular junction. Nat. Neurosci. *2*, 791–797.

22. Liu, Q., Chen, B., Yankova, M., Morest, D.K., Maryon, E., Hand, A.R., Nonet, M.L., and Wang, Z.W. (2005). Presynaptic ryanodine receptors are required for normal quantal size at the *Caenorhabditis elegans* neuromuscular junction. J. Neurosci. *25*, 6745–6754.

23. Xue, M., Craig, T.K., Xu, J., Chao, H.T., Rizo, J., and Rosenmund, C. (2010). Binding of the complexin N terminus to the SNARE complex potentiates synaptic-vesicle fusogenicity. Nat. Struct. Mol. Biol. *17*, 568–575.

24. Xue, M., Reim, K., Chen, X., Chao, H.T., Deng, H., Rizo, J., Brose, N., and Rosenmund, C. (2007). Distinct domains of complexin I differentially regulate neurotransmitter release. Nat. Struct. Mol. Biol. *14*, 949–958.

25. Frøkjaer-Jensen, C., Davis, M.W., Hopkins, C.E., Newman, B.J., Thummel, J.M., Olesen, S.P., Grunnet, M., and Jorgensen, E.M. (2008). Single-copy insertion of transgenes in *Caenorhabditis elegans*. Nat. Genet. *40*, 1375–1383.

26. Martin, J.A., Hu, Z., Fenz, K.M., Fernandez, J., and Dittman, J.S. (2011). Complexin has opposite effects on two modes of synaptic vesicle fusion. Curr. Biol. *20*, this issue, 97–105.

27. Cho, R.W., Song, Y., and Littleton, J.T. (2010). Comparative analysis of *Drosophila* and mammalian complexins as fusion clamps and facilitators of neurotransmitter release. Mol. Cell. Neurosci. *45*, 389–397.

28. Miller, K.G., Alfonso, A., Nguyen, M., Crowell, J.A., Johnson, C.D., and Rand, J.B. (1996). A genetic selection for *Caenorhabditis elegans* synaptic transmission mutants. Proc. Natl. Acad. Sci. USA *93*, 12593–12598.

29. Liu, Q., Hollopeter, G., and Jorgensen, E.M. (2009). Graded synaptic transmission at the *Caenorhabditis elegans* neuromuscular junction. Proc. Natl. Acad. Sci. USA *106*, 10823–10828.

30. Rostaing, P., Weimer, R.M., Jorgensen, E.M., Triller, A., and Bessereau, J.L. (2004). Preservation of immunoreactivity and fine structure of adult *C. elegans* tissues using high-pressure freezing. J. Histochem. Cytochem. *52*, 1–12.

31. McDonald, K.L., and Auer, M. (2006). High-pressure freezing, cellular tomography, and structural cell biology. Biotechniques *41*, 137, 139, 141 passim.

32. Hammarlund, M., Palfreyman, M.T., Watanabe, S., Olsen, S., and Jorgensen, E.M. (2007). Open syntaxin docks synaptic vesicles. PLoS Biol. *5*, e198.

33. Waterhouse, A.M., Procter, J.B., Martin, D.M.A., Clamp, M., and Barton, G.J. (2009). Jalview Version 2—a multiple sequence alignment editor and analysis workbench. Bioinformatics *25*, 1189–1191.
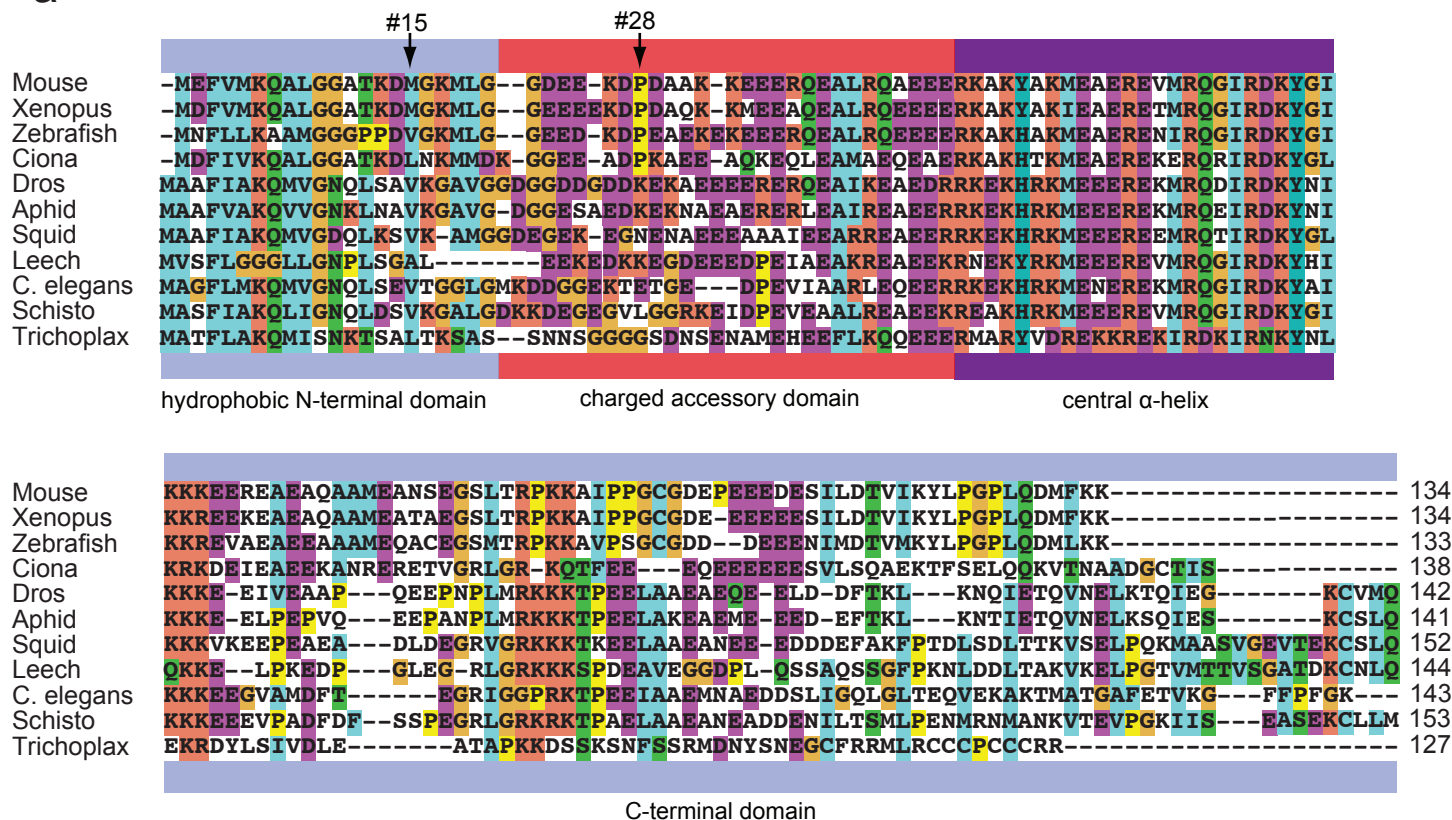
# Supplemental Information

# Complexin Maintains Vesicles

# in the Primed State in *C. elegans*

Robert J. Hobson, Qiang Liu, Shigeki Watanabe, and Erik M. Jorgensen

a

#15          #28

| | | |
|---|---|---|
| Mouse | -MEFVMKQALGGATKDMGKMLG | GDEE-KDPDAAK-KEEEERQEALRQAEEERKAKYAKMEAEREVMRQGIRDKYGI |
| Xenopus | -MDFVMKQALGGATKDMGKMLG | GEEEEKDPDAQK-KMEEAQEALRQEEEERKAKYAKIEAERETMRQGIRDKYGI |
| Zebrafish | -MNFLLKAAMGGGPPDVGKMLG | GEED-KDPEAEKEKEEEERQEALRQEEEERKAKHAKMEAERENIRQGIRDKYGI |
| Ciona | -MDFIVKQALGGATKDLNKMMDK | GGEE-ADPKAEE-AQKEQLEAMAEQEAERKAKHTKMEAEREKERQRIRDKYGL |
| Dros | MAAFIAKQMVGNQLSAVKGAVGGDGGDDGDDKEKAEEEEERQEAIKEAEDRRKEKHRKMEEEREKMRQDIRDKYNI |
| Aphid | MAAFVAKQVVGNKLNAVKGAVG-DGGESAEDKEKNAEAEERLEAIREAEERRKEKHRKMEEEREKMRQEIRDKYNI |
| Squid | MAAFIAKQMVGDQLKSVK-AMGGDEGEK-EGNENAEEEAAAIEEARREAEEERRKEKHRKMEEEREEMRQTIRDKYGL |
| Leech | MVSFLGGGLLGNPLSGAL-------EEKEDKKEGDEEEDPEIAAEAKREAEEKRNEKYRKMEEEREVMRQGIRDKYHI |
| C. elegans | MAGFLMKQMVGNQLSEVTGGLGMKDDGGEKTETGE---DPEVIAARLEQEERRKEKHRKMENEREKMRQGIRDKYAI |
| Schisto | MASFIAKQLIGNQLDSVKGALGDKKDEGEGVLGGRKEIDPEVEAALREAEEKREAKHRKMEEEREVMRQGIRDKYGI |
| Trichoplax | MATFLAKQMISNKTSALTKSAS--SNNSGGGGSDNSENAMEHEEFLKQQEEERMARYVDREKKREKIRDKIRNKYNL |

hydrophobic N-terminal domain          charged accessory domain          central α-helix

| | | |
|---|---|---|
| Mouse | KKKEEREAEAQAAMEANSEGSLTRPKKAIPPGCGDEPEEEDESILDTVIKYLPGPLQDMFKK------------------ | 134 |
| Xenopus | KKREEKEAEAQAAMEATAEGSLTRPKKAIPPGCGDE-EEEEESILDTVIKYLPGPLQDMFKK------------------ | 134 |
| Zebrafish | KKREVAEAEEAAAMEQACEGSMTRPKKAVPSGCGDD--DEEENIMDTVMKYLPGPLQDMLKK----------------- | 133 |
| Ciona | KRKDEIEAEEKANRERETVGRLGR-KQTFEE---EQEEEEEESVLSQAEKTFSELQQKVTNAADGCTIS---------- | 138 |
| Dros | KKE-EIVEAAP---QEEPNPLMRKKKTPEELAAEAQE-ELD-DFTKL---KNQIETQVNELKTQIEG--------KCVMQ | 142 |
| Aphid | KKKE-ELPEPVQ---EEPANPLMRKKKTPEELAKEAEME-EED-EFTKL---KNTIETQVNELKSQIES--------KCSLQ | 141 |
| Squid | KKKVKEEPEAEA---DLDEGRVGRKKKTKEELAAEANEE-EDDDEFAKFPTDLSDLTTKVSELPQKMAASVGEVTEKCSLQ | 152 |
| Leech | QKKE--LPKEDP---GLEG-RLGRKKKSPDEAVEGGDPL-QSSAQSSGFPKNLDDLTAKVKELPGTVMTTVSGATDKCNLQ | 144 |
| C. elegans | KKKEEGVAMDFT-----EGRIGGPRKTPEEIAAEMNAEDDSLIGQLGLTEQVEKAKTMATGAFETVKG---FFPFGK--- | 143 |
| Schisto | KKKEEEVPADFDF--SSPEGRLGRKRKTPAELAAEANEADDENILTSMLPENMRNMANKVTEVPGKIIS---EASEKCLLM | 153 |
| Trichoplax | EKRDYLSIVDLE-------ATAPKKDSSKSNFSSRMDNYSNEGCFRRMLRCCCPCCCRR--------------------- | 127 |

C-terminal domain

b

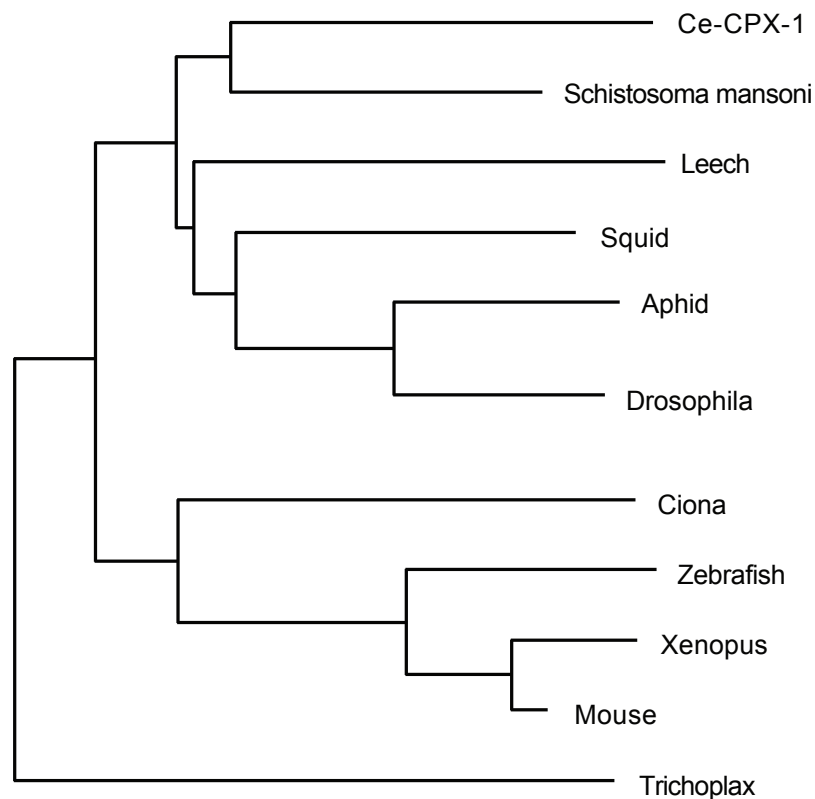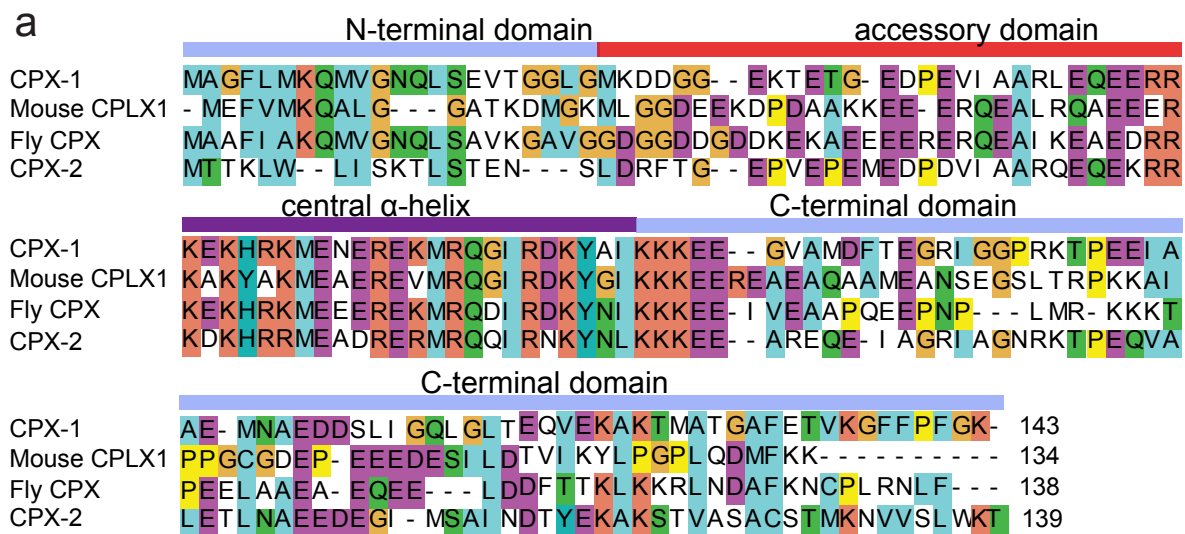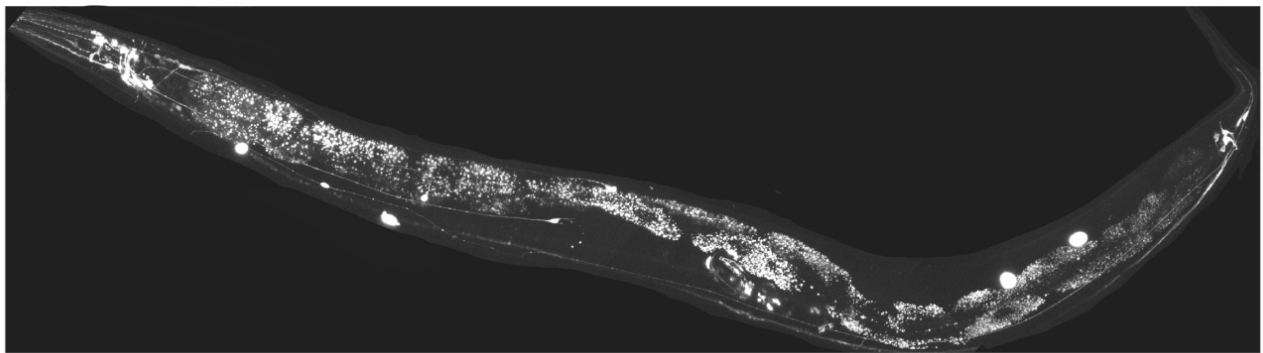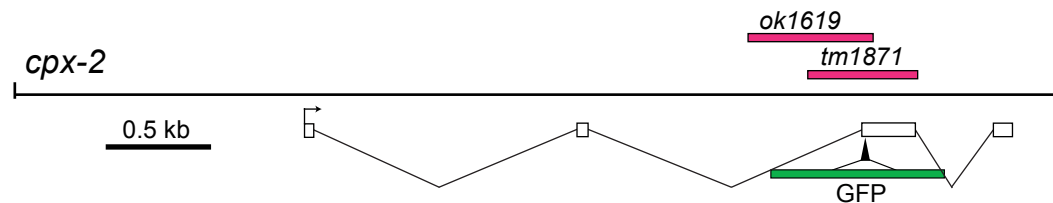| | |
|---|---|
| | Ce-CPX-1 |
| | Schistosoma mansoni |
| | Leech |
| | Squid |
| | Aphid |
| | Drosophila |
| | Ciona |
| | Zebrafish |
| | Xenopus |
| | Mouse |
| | Trichoplax |

**Figure S1. The Complexin Family**

(a) Multiple sequence alignment of complexins from species representing diverse phyla. The domains of complexin are defined based on sequence conservation. The N-terminal domain is hydrophobic and some residues are conserved across phyla.  The accessory domain is poorly conserved but is highly charged, comprised mostly of negatively-charged glutamates.  In our alignment we have extended the accessory domain to include the entire charged sequence after the proline (#28) present in vertebrates. The accessory domain, originally called the accessory helix, contains a helix-disrupting proline in chordates, annelids, nematodes and platyhelminths. Between the N-terminal hydrophobic domain and the charged accessory domain are several conserved glycine residues, suggesting that these two domains may be connected by a flexible hinge. The central helix binds to the SNARE complex and is highly conserved.  The C-terminal domain is poorly conserved apart from the distribution of charged motifs.  Most organisms express genes or splice forms containing a 'CAAX' prenylation site at the very carboxy terminus (not all CAAX-containing forms are shown).  *C. elegans* oddly does not encode a CAAX-containing variant.
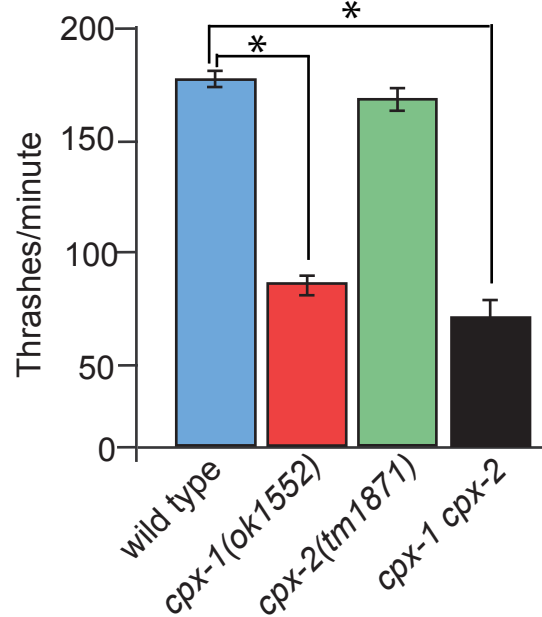
(b) Phylogenetic tree based on a multiple sequence alignment of complexin isoforms. All alignments were produced by ClustalW2 and the tree was produced using Njplot. The following sequences were used for the alignment: mouse complexin-1 GI 227330544, *Drosophila melanogaster* complexin-1 GI 7769722, *Schistosoma mansoni* GI 256080104, Aphid GI 253683501, Squid GI 14717828, Leech GI 25264681, *Xenopus laevis* GI 148224652, Zebrafish GI 50539986, *Trichoplax* GI 190580758, *Ciona intestinalis* GI 198438415, *C. elegans* CPX-1 GI 17510617.

a

N-terminal domain          accessory domain

```
CPX-1        MAGFLMKQMVGNQLSEVTGGLGMKDDGG--EKTETG-EDPEVIAARLEQEERR
Mouse CPLX1  -MEFVMKQALG---GATKDMGKMLGGDEEKDPDAAKKEE-ERQEALRQAEEER
Fly CPX      MAAFIAKQMVGNQLSAVKGAVGGDGGDGDDKEKAEEEERERQEAIKEAEDRR
CPX-2        MTTKLW--LISKTLSTEN---SLDRFTG--EPVEPEMEDPDVIAARQEQEKRR
```

central α-helix          C-terminal domain

```
CPX-1        KEKHRKMENEREKMRQGIRDKYAIKKKEE--GVAMDFTEGRIGGPRKTPEEIA
Mouse CPLX1  KAKYAKMEAEREVMRQGIRDKYGIKKKEEREAEAQAAMEANSEGSLTRPKKAI
Fly CPX      KEKHRKMEEEREKMRQDIRDKYNIKKKEE-IVEAAPQEEPNP---LMR-KKKT
CPX-2        KDKHRRMEADRERMRQQIRNKYNLKKKEE-AREQE-IAGRIAGNRKTPEQVA
```

C-terminal domain

```
CPX-1        AE-MNAEDDSLIGQLGLTEQVEKAKTMATGAFETVKGFFPFGK-    143
Mouse CPLX1  PPGCGDEP-EEEDESILDTVIKYLPGPLQDMFKK---------    134
Fly CPX      PEELAAEA-EQEE---LDDFTTKLKKRLNDAFKNCPLRNLF--    138
CPX-2        LETLNAEEDEGI-MSAINDTYEKAKSTVASACSTMKNVVSLWKT    139
```
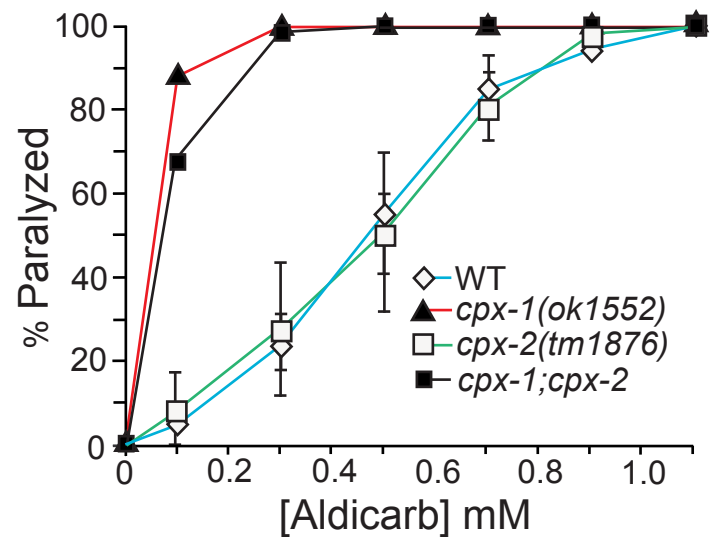
b



c



d

**Figure S2.**

(a). *cpx-2* is not highly conserved with other complexins in the N-terminal or accessory domains. CPX-2 was aligned with *C. elegans* CPX-1, mouse CplxI (AAH14803) and *Drosophila* CPX (AAF69518) using ClustalW2.

(b). *cpx-2* is expressed in the nervous system. Above, gene model and regions deleted in *C. elegans* complexin mutants. Red bars indicate regions deleted in the mutants. The black line represents the region of the genome used to create the GFP construct. Below, a reporter construct consisting of the *cpx-2* gene fused with GFP is expressed in approximately 30 head, midbody and tail neurons and the coelomocytes. Images were taken with a confocal microscope and are of young adult hermaphrodites oriented dorsal up, and anterior to the left. Images are a stitch of multiple confocal Z-projections along the length of the animal.

(c). *cpx-2* mutants are not defective for thrashing in liquid and *cpx-1 cpx-2* (EG4228) double mutants are not worse than *cpx-1(ok1552)*. Two-tailed unpaired T-tests: * $P<0.0005$.

(d). *cpx-2* mutants are not hypersensitive to aldicarb and *cpx-1 cpx-2* double mutants are not worse than *cpx-1* single mutants.
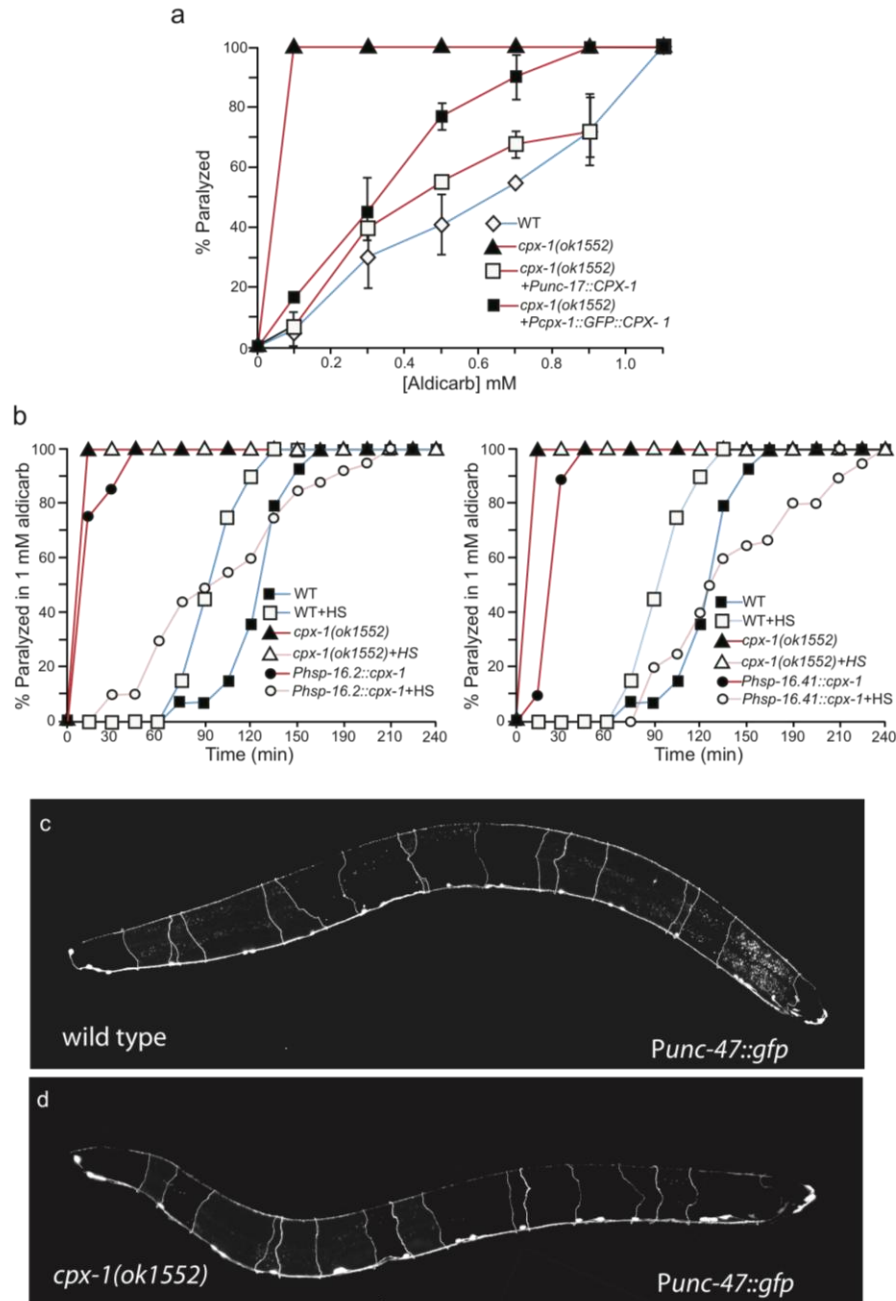
**Figure S3.**

(a) *cpx-1(ok1552)* aldicarb hypersensitivity can be rescued by expressing *cpx-1* in the acetylcholine motor neurons using the *unc-17* promoter (P*unc-17::cpx-1(+)* EG4713). The N-terminally GFP-tagged CPX-1 is also capable of rescuing the aldicarb phenotype of *cpx-1(ok1552)* mutants (P*cpx-1::GFP::cpx-1* EG4407).

(b) Complexin is required for synaptic function but not development. Wild-type complexin was expressed in a *cpx-1(ok1552)* mutant adult using a heatshock promoter. Hypersensitivity to the acetylcholinesterase inhibitor aldicarb was rescued after heatshock (HS). Animals were incubated at 34°C for one hour, then placed at 20-22°C for six hours prior to the assay. Two different heat-shock promoters were used P*hsp-16.2* and P*hsp-16.41* with similar results for both.

4

(c, d) Axon outgrowth is normal in *cpx-1* mutants. (a) Wild-type animals expressing P*unc-25::GFP* (*oxIs12*) and (b) *cpx-1(ok1552) oxIs12* animals were imaged with a confocal microscope. The *unc-25* promoter drives expression in all GABA neurons. The normal number and distribution of GABA neuron commissures are observed in *cpx-1* mutants. Young adult hermaphrodites are oriented dorsal to the top and anterior to the right. Images are a stitch of multiple confocal Z-projections along the length of the animal.
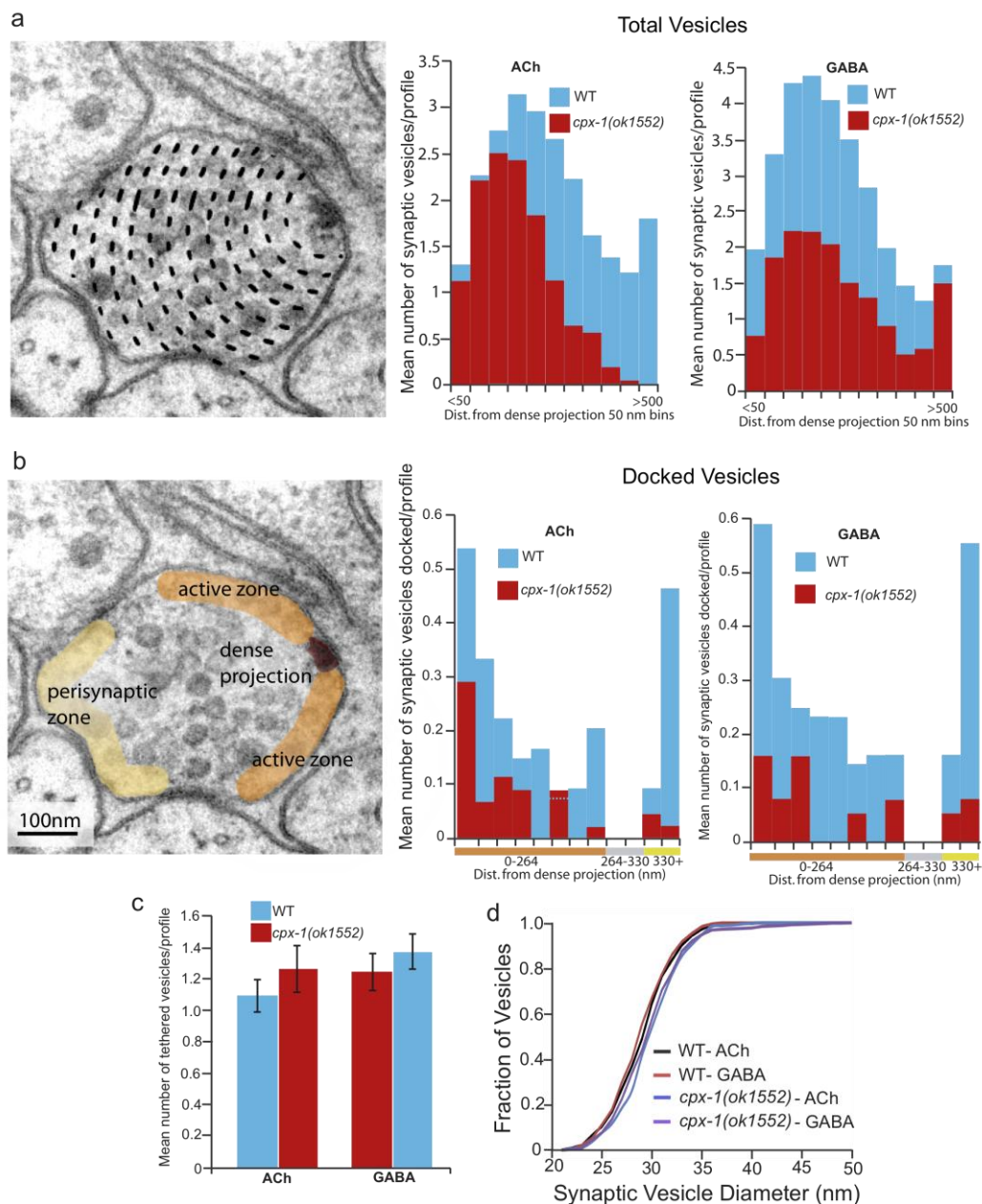
**Figure S4. The Distribution of Synaptic Vesicles at the Synapse**
(a). Cytoplasmic distribution. Synaptic vesicles in the cytoplasm cluster around the dense projection. The distribution of vesicles within acetylcholine and GABA neuromuscular junctions in *cpx-1(ok1552)* appears normal. *Left,* An example of the 50 nm bins used for the analysis of synaptic vesicle distribution. Concentric rings were drawn around the dense projection and the distance of each vesicle from the dense projection was determined. *Right,* Graph of the distribution of all synaptic vesicles. Each bar represents the number of vesicles within a 50 nm bin from the dense projection.
(b). Plasma membrane distribution. *Left,* An illustration of the plasma membrane zones at a neuromuscular junction. The orange band identifies the active zone that flanks the dense projection. The active zone is where synaptic vesicles dock and fuse with the plasma membrane, and is juxtaposed to the postsynaptic target. Docking at the active zone is usually found within 264 nm of the dense projection. There is a region from 264 to 330 nm in which

6

vesicles are not docked (gray).  The yellow band indicates the perisynaptic zone. *Right,* Each bar represents the number of vesicles touching the plasma membrane along the active zone in 33 nm bins from the dense projection.
(c) The number of vesicles tethered to the plasma membrane (vesicles that are attached to the plasma membrane by a filament) is normal in a *cpx-1(ok1552)* mutant.
(d). Vesicle diameters are normal in *complexin-1* mutants.  Cumulative plot of synaptic vesicle diameters at the synapse.
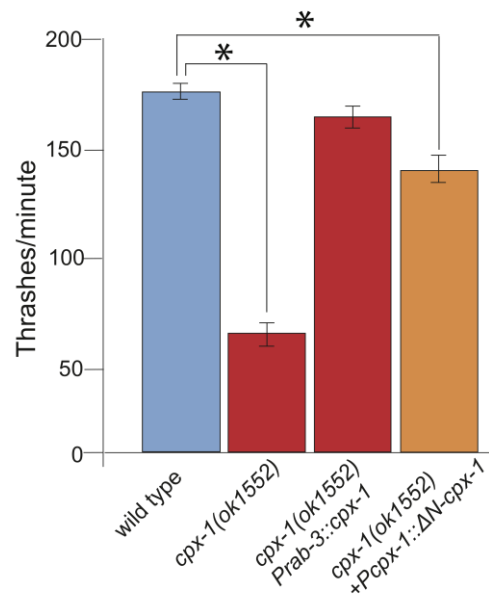


**Figure S5. Deletion of the N-Terminus Partially Rescues Thrashing Behavior**
The ΔN-*cpx-1* construct (EG6182) largely rescues *cpx-1(ok1552)* thrashing behavior. *Tukey-Kramer-test: *P*<0.001.

## Supplemental Experimental Procedures

### Reporter Constructs

All primers used are listed in Supplementary Table 1 *cpx-1*: To create a translational GFP reporter construct, the 5' end of the *cpx-1* gene including 1.0 kb of the promoter and the first three codons, was amplified by PCR with the primers oRJH1 and oRJH2. The primers contained restriction sites for *PstI* and *AgeI* that were subsequently used to subclone the PCR product upstream of GFP in the vector pPD117.01. The 3' end of the gene including the rest of the *cpx-1* coding region and the 3'UTR was amplified by PCR with the following primers oRJH3 and oRJH4 containing restriction sites *EcoRI* and *NgoMIV* and subcloned downstream of GFP in the same vector to make fusion protein. The final construct was pRH7 P*cpx-1::GFP::CPX-1*.

*cpx-2:* To create a translational GFP reporter construct, the 5' end of the *cpx-2* gene including 1.1 kb promoter sequence was amplified with the primers oRJH5 and oRJH6 containing restriction sites for *PstI* and *KpnI*. The resulting PCR product was subcloned upstream of GFP in the vector pPD117.01 to make a fusion construct. The 3' end of *cpx-2* including the rest of the coding region and the 3'UTR was amplified with the following primers oRJH7 and oRJH8 containing the restriction sites *EcoRI* and *NgoMIV* and subcloned downstream of GFP in the same vector. The final construct was P*cpx-2::GFP::CPX-2*.

### Rescuing Constructs

The *cpx-1* gene was amplified by PCR from *C. elegans* genomic DNA from the ATG to the stop codon using the primers oRJH9 and oRJH10. These primers also contained *attB* recombination arms so the resulting amplification product could be recombined with the donor vector pDONR221 (Invitrogen) using BP Clonase II (Invitrogen) to produce the pEntry[1-2][*cpx-1*] minigene. The same reaction was used to create the N-terminal truncation mutant except the primers used for amplification were oRJH11 and oRJH12. This created the Gateway entry clone (Invitrogen) pEntry[1-2][ΔN-*cpx-1*].

The *cpx-1* promoter was amplified from genomic DNA using the primers RJH13 and oRJH14 and subsequently recombined with the pDONR P4-P1R (Invitrogen) vector. This created the Gateway entry clone (Invitrogen) pEntry[4-1][P*cpx-1*] vector. 3.2 kb of the acetylcholine neuron promoter *unc-17* was amplified by PCR from genomic DNA using the following primers oRJH15 and oRJH16 and subsequently recombined with the pDONR P4-P1R (Invitrogen) vector. This created the Gateway entry clone (Invitrogen) pEntry[4-1][P*unc-17*] vector. The *cpx-1* 3'UTR was amplified by PCR from genomic DNA using the following primers oRJH17 and oRJH18 and subsequently recombined with the pDONR P2-P3R (Invitrogen) vector. This created the Gateway entry clone (Invitrogen) pEntry[2-3][*cpx-1*_3'UTR]. The pEntry[4-1] pan-neuronal *rab-3* promoter (pEGB05) and the pEntry[2-3][*unc-54*_UTR] were previously generated in the Jorgensen lab. To generate *cpx-1* expression clones the plasmids pEntry[4-1][P*rab-3*] or, pEntry[4-1][P*unc-17*], pEntry[2-3][*unc-54* 3'UTR] were recombined with the Gateway destination vector pDest R4-R3 (Invitrogen) using the LR Clonase II recombinase (Invitrogen). The following expression clones were created: pExp[P*rab-3::CPX-1::unc-54*] and pExp[P*unc-17::CPX-1::unc-54*].

To create MosSCI [1] expression constructs for *cpx-1* and ΔN-*cpx-1* the pEntry[4-1][P*cpx-1*], pEntry[1-2][*cpx-1*] or pEntry[1-2][ΔN-*cpx-1*] and the pEntry[2-3][*cpx-1*_3'UTR] were recombined with the MosSCI targeting vector pCFJ150 using the LR Clonase II recombinase (Invitrogen). The following MosSCI targeting vectors were created: pExp5605[P*cpx-1::CPX-1::cpx-1*_3'UTR] pExp5605[P*cpx-1::*ΔN-*CPX-1::cpx-1_3'UTR*].

To create heat-shock inducible *cpx-1* transgene the pEntry[1-2][*cpx-1*], pEntry[2-3][*let-858*_3'UTR] and pDest P4-P1R were recombined with either the pCM1.56 (pEntry[4-1][P*hsp-16-2*]) or the pCM1.57 (pEntry[4-1][P*hsp-16-41*]) heat-shock promoters. The following constructs were made: pExp[P*hsp-16-2::CPX-1::let-858_UTR*] and pExp[P*hsp-16-41::CPX-1::let-858_UTR*]

**Strains**

N2 Bristol was used as the wild type in all experiments. EG4662 *cpx-1(ok1552)* was out-crossed four times against N2. The *ok1552* breakpoint was confirmed by amplifying across the deletion and sequencing the resulting PCR products. EG4227 *cpx-2(tm1871)* was out-crossed four times against N2. EG4228 *cpx-1(ok1552); cpx-2(tm1871).* MT8247 *lin-15(n765ts) nIs52[Punc-25::SNB-1:GFP; lin-15(+)].* ZM54 *hpIs3[Punc-25::SYD-2:GFP].* EG6153 *oxIs22[Punc-49::UNC-49b:GFP].* EG4935 *cpx-1(ok1552); nIs52.* EG4934 *cpx-1(ok1552); hpIs3.* EG6201 *cpx-1(ok1552); oxIs22.* EG4361 *lin-15(n765ts); oxEx844[lin-15(+); Pcpx-1::GFP::CPX-1]* The extrachromosomal array *oxEx844* was generated by injecting 20 ng/$\mu$l pRH7 and 80 ng/$\mu$l *lin-15(+)* rescuing DNA into *lin-15(n765ts)* to generate the strain EG4361. EG4362 *lin-15(n765ts); oxEx845[lin-15(+);Pcpx-2::GFP::CPX-2]* The extrachromosomal array *oxEx845* was generated by injecting 20 ng/$\mu$l pRH9 and 80 ng/$\mu$l *lin-15(+)* rescuing DNA into *lin-15(n765ts)* to generate the strain EG4362. EG4633 *cpx-1(ok1552); oxEx993[Prab-3::cpx-1::unc-54].* This strain was created by injecting 20 ng/$\mu$l P*rab-3::CPX-1::unc-54* and 80 ng/$\mu$l 1 kb DNA ladder (Promega) into *cpx-1(ok1552)* animals. EG4713 *cpx-1(ok1552); oxEx1033[Punc-17::CPX-1::unc-54].* This strain was created by injecting 20 ng/$\mu$l P*unc-17::CPX-1::unc-54* and 80 ng/$\mu$l 1 kb DNA ladder (Promega) into *cpx-1(ok1552)* animals.

**Single Copy Transgene Insertions**

EG6182 *cpx-1(ok1552); oxSi264[Pcpx-1:: ΔN-CPX-1 unc-119(+)].* EG6317 *cpx-1(ok1552); oxSi301[Pcpx-1::CPX-1::cpx-1_3'UTR unc-119(+)].* These strains were created by inserting the P*cpx-1::CPX-1* and the *Pcpx-1::ΔN-CPX-1* transgene into the *C. elegans* genome by *Mos1*-mediated single copy insertion (MosSCI) as previously described [1]. Briefly, *unc-119(ed3)* III mutants containing *ttTi5605* II (EG4322) were injected with a mixture of plasmids containing the *Mos1* transposase, the targeting vectors, pExp5605[*Pcpx-1::CPX-1::cpx-1_3'UTR*] or pExp5605[*Pcpx-1:: ΔN-CPX-1::cpx-1_3'UTR unc-119(+)*], and mCherry fluorescent markers expressed in muscles and neurons to mark extrachromosomal arrays. Offspring of the injected animals were selected in later generations for homozygous *unc-119* rescue. This MosSCI was crossed into *cpx-1(ok1552)* mutants using standard methods.

**Thrashing Assays**

Thrashing assays were performed as previously described [2]. Briefly, L4 animals were picked one day prior to assay, and allowed to grow for 24 hours at 22-25°C. Individual animals were placed in an 80 $\mu$l drop of M9 solution on an unseeded portion of an NGM plate and left for one minute to recover from transfer. After recovery, the number of thrashes was counted for 90 seconds. One 'thrash' was defined as a change in direction of bending in the middle of the animal; in other words the head pointed to the right, to the left, and then to the right again is counted as two thrashes. At least 12 individuals were tested for each genotype.

## Aldicarb Assays

Aldicarb plates were made by adding the required volume of 100 mM aldicarb (in 95% ethanol) to molten (55°C) NGM. The agar was poured into 5 cm plates. When the NGM had solidified 50 μl of a liquid culture of OP50 *E. coli* was added to the plates and allowed to dry overnight. The plates were stored at 4°C until use. For the assays, 20-25 worms were added to the center of room-temperature aldicarb plates and scored for paralysis after four hours. The assay was performed in triplicate for each genotype at each concentration of aldicarb. For heat-shock experiments, strains were heat shocked for one hour at 34°C and then allowed to recover at room temperature for six hours prior to assay. For heat shock aldicarb assays, 20-25 worms were added to plate containing 1 mM aldicarb and scored for paralysis every fifteen minutes. The acute assay was performed in triplicate for each genotype. Paralysis in both assays was scored as the lack of movement in response to prodding with a platinum wire. The assayer was blind to the genotype of the each strain prior to assay.

## Confocal Microscopy

Worms were immobilized in 2% phenoxypropanol in M9 solution on freshly made 2% agarose pads. Images were acquired on a Pascal LSM5 confocal microscope (Zeiss, Inc.) with a 63x 1.4NA oil objective. For imaging of the dorsal nerve cord worms were imaged with the dorsal surface facing towards the objective. For each of the synaptic markers a Z-stack was taken of a 70 μm section of nerve cord and the total number of GFP positive puncta were counted.

## Electrophysiology

Young adult hermaphrodite animals were used for electrophysiological analysis. Miniature and evoked postsynaptic currents (mPSCs and ePSCs) at the neuromuscular junction were recorded as previously described [3,4]. In brief, an animal was immobilized on a Sylgard-coated glass coverslip by applying a cyanoacrylate adhesive along the dorsal side. A longitudinal incision was made in the dorsolateral region. The cuticle flap was folded back and glued to the coverslip, exposing the ventral nerve cord and two adjacent muscle quadrants. A microscope (Axioskop; Carl Zeiss, Inc.) equipped with a 40x water immersion lens and 15x eyepieces was used for viewing the preparation. Borosilicate glass pipettes with a tip resistance of ~3–5 MΩ were used as electrodes for voltage clamping. The classical whole-cell configuration was obtained by rupturing the patch membrane of a gigaohm seal formed between the recording electrode and a body wall muscle cell. The cell was voltage clamped at ~-60 mV to record mPSCs and ePSCs. ePSCs were evoked by applying a 0.5-ms square wave current pulse at a supramaximal voltage (25 V) through a stimulation electrode placed in close apposition to the ventral nerve cord. Postsynaptic currents were amplified (EPC10; HEKA) and acquired with Patchmaster software (HEKA). Data were sampled at a rate of 10 kHz after filtering at 2 kHz. The recording pipette solution contained the following: 120 mM KCl, 20 mM KOH, 5 mM TES, 0.25 mM $CaCl_2$, 4 mM $MgCl_2$, 36 mM sucrose, 5 mM EGTA, and 4 mM $Na_2ATP$; pH adjusted to 7.2 with KOH and osmolarity to 310–320 mOsm. The standard external solution included the following: 150 mM NaCl, 5 mM KCl, 5 mM $CaCl_2$, 1 mM $MgCl_2$, 5 mM sucrose, 10 mM glucose, and 15 mM Hepes; pH adjusted to 7.35 with NaOH with osmolarity 330–340 mOsm. In experiments where the calcium concentration was changed the following external solutions were used: (1mM calcium solution) 150 mM NaCl, 5 mM KCl, 1 mM $CaCl_2$, 1 mM $MgCl_2$, 5 mM sucrose, 10 mM glucose, and 15 mM Hepes; (0.4 mM calcium solution) 150 mM NaCl, 5 mM KCl, 0.4 mM $CaCl_2$, 1 mM $MgCl_2$, 5 mM sucrose, 10 mM glucose, and 15 mM Hepes; (0 mM calcium solution) 150 mM NaCl, 5 mM KCl, 6 mM $MgCl_2$, 5 mM sucrose, 10 mM glucose, and 15 mM Hepes.

Amplitude and frequency of mPSCs were analyzed using MiniAnalysis (Synaptosoft). A detection threshold of 10 pA was used in initial automatic analysis, followed by visual inspections to include missed events (≥5 pA) and to exclude false events resulting from baseline fluctuations. Amplitudes of ePSCs were measured with Fitmaster (HEKA). The amplitude of the largest peak of ePSCs from each experiment was used for statistical analysis. Data were imported into Origin, version 7.5 (OriginLab), for graphing and statistical analysis. Unpaired t-test was used for statistical comparisons. A *P* value of < 0.05 is considered statistically significant.

**Electron Microscopy**

N2 and *cpx-1(ok1552)* worms were fixed in parallel for electron microscopy using high-pressure freezing followed by substitution of solvent-based fixatives as previously described [5-7]. Briefly, ten animals were placed into a freezing chamber (100-um well of type A specimen carrier) filled with bacteria, covered with a type B specimen carrier flat side down, and frozen instantaneously in the BAL-TEC HPM 010 (BAL- TEC, http://www.bal-tec.com). Frozen animals were fixed in a Leica EM AFS system (http://www.leica.com) with 0.5% glutaraldehyde and 0.1% tannic acid in anhydrous acetone for 4 d at -90°C, followed by 2% osmium tetroxide in anhydrous acetone for 38.9 h with gradual temperature increases (constant temperature at -90°C for 7 h, 5°C/h to 25°C over 13 h, constant temperature at 25°C for 16 h, and 10°C/h to 4°C over 2.9 h). Fixed animals were embedded in araldite resin (30% araldite/acetone for 4 h, 70% araldite/acetone for 5 h, 90% araldite/acetone overnight, and pure araldite for 8 h). Ribbons of ultrathin (33 nm) serial sections were collected using an ultracut E microtome. Images were obtained on a Hitachi H-7100 electron microscope (http://www. hitachi.com) using a Gatan (http://www.gatan.com) digital camera. A total of 250 ultrathin contiguous sections were cut and the ventral nerve cord reconstructed from two animals representing each genotype. Image analysis was performed using ImageJ software (http:// rsb.info.nih.gov/ij).

All morphometry was conducted blind to genotype and included a matched wild-type worm that was fixed in parallel. The number of synaptic vesicles (~30 nm in diameter) in each synaptic profile was counted, and their distances from the dense projection and plasma membrane were measured. Docked vesicles were defined as touching the plasma membrane. Analysis included the acetylcholine neurons VA and VB and the GABA neuron VD.

**Reagents**

All chemicals were purchased from Sigma-Aldrich and all molecular reagents from Invitrogen and New England Biolabs, unless otherwise stated.

**Table S1.**

| Primer Name | Sequence |
|---|---|
| oRJH1 | AAAACTGCAGGGGTAGATTTACGGCGCGTGTC |
| oRJH2 | AGTCAAACCGGTAAGCCCGCCATTTTTCACGTTTTG |
| oRJH3 | GCCGCCGGCCTGACTACGTATGGTTAAGAACGTGC |
| oRJH4 | CCGGAATTCATGAAACAAATGGTCGGAAATCAGC |
| oRJH5 | AAAACTGCAGGGCATTAAATAACCACAAGATCGAC |
| oRJH6 | CGGGGTACCGCCTCACGATCGGCTTCCATTCTTC |
| oRJH7 | CCGGAATTCCGTATGCGTCAGCAAATCCGG |
| oRJH8 | GCCGCCGGCATAGCTCGTGACAGCCCGTCAAAC |
| oRJH9 | GGGGACAAGTTTGTACAAAAAAGCAGGCTAAAATGGCGGGCTTTTTGATGAAAC |
| oRJH10 | GGGGACCACTTTGTACAAGAAAGCTGGGTTTATTTTCCAAATGGGAAGAATCC |
| oRJH11 | GGGGACAAGTTTGTACAAAAAAGCAGGCTAAAAATGGTGACCGGCGGTCTC |
| oRJH12 | GGGGACCACTTTGTACAAGAAAGCTGGGTTTATTTTCCAAATGGGAAGAATCC |
| oRJH13 | GGGGACAACTTTGTATAGAAAGTTGGAAATTACTTTTGGTGTATTATTGCTGTGC |
| oRJH14 | GGGGACTGCTTTTTTGTACAAACTTGTTTTCACGTTTTGTTTTGAGGGTTTC |
| oRJH15 | GGGGACAACTTTGTATAGAAAGTTGTACACCAATCATTTCTCCCCTCCG |
| oRJH16 | GGGGACTGCTTTTTTGTACAAACTTGTTTTGAACAAGAGATGCGGAAAATAGAAAG |
| oRJH17 | GGGGACAGCTTTCTTGTACAAAGTGGATTATGACAAATGACAAAAAATTGTCTCTC |
| oRJH18 | GGGGACAACTTTGTATAATAAAGTTGTATCTGTTTTCTCACGGGTTTAGG |

**Supplemental References**

[1] C. Frøkjaer-Jensen, M.W. Davis, C.E. Hopkins, B.J. Newman, J.M. Thummel, S. Olesen, et al., Single-copy insertion of transgenes in Caenorhabditis elegans, Nat. Genet. 40 (2008) 1375-1383.

[2] K.G. Miller, A. Alfonso, M. Nguyen, J.A. Crowell, C.D. Johnson, J.B. Rand, A genetic selection for Caenorhabditis elegans synaptic transmission mutants, Proc. Natl. Acad. Sci. U.S.A. 93 (1996) 12593-12598.

[3] J.E. Richmond, E.M. Jorgensen, One GABA and two acetylcholine receptors function at the C. elegans neuromuscular junction, Nat. Neurosci. 2 (1999) 791-797.

[4] Q. Liu, G. Hollopeter, E.M. Jorgensen, Graded synaptic transmission at the Caenorhabditis elegans neuromuscular junction, Proc. Natl. Acad. Sci. U.S.A. 106 (2009) 10823-10828.

[5] P. Rostaing, R.M. Weimer, E.M. Jorgensen, A. Triller, J. Bessereau, Preservation of immunoreactivity and fine structure of adult C. elegans tissues using high-pressure freezing, J. Histochem. Cytochem. 52 (2004) 1-12.

[6] K.L. McDonald, M. Auer, High-pressure freezing, cellular tomography, and structural cell biology, BioTechniques. 41 (2006) 137, 139, 141 passim.

[7] M. Hammarlund, M.T. Palfreyman, S. Watanabe, S. Olsen, E.M. Jorgensen, Open syntaxin docks synaptic vesicles, PLoS Biol. 5 (2007) e198.